



## ORIGINAL ARTICLE

# Tracing plant source water dynamics during drought by continuous transpiration measurements: An in-situ stable isotope approach

Angelika Kübert<sup>1,2</sup>  | Maren Dubbert<sup>3</sup> | Ines Bamberger<sup>4</sup> |  
Kathrin Kühnhammer<sup>1,5</sup> | Matthias Beyer<sup>5</sup> | Joost van Haren<sup>6,7</sup> | Kinzie Bailey<sup>8</sup> |  
Jia Hu<sup>8</sup> | Laura K. Meredith<sup>6,8</sup> | S. Nemiah Ladd<sup>1,9</sup> | Christiane Werner<sup>1</sup> 

<sup>1</sup>Ecosystem Physiology, University of Freiburg, Freiburg, Germany

<sup>2</sup>Institute for Atmospheric and Earth System Research, University of Helsinki, Helsinki, Finland

<sup>3</sup>Isotope Biogeochemistry and Gas Fluxes, Landscape Functioning, ZALF, Müncheberg, Germany

<sup>4</sup>Atmospheric Chemistry Group, University of Bayreuth, Bayreuth, Germany

<sup>5</sup>Institute for Geoecology, Technical University of Braunschweig, Braunschweig, Germany

<sup>6</sup>Biosphere 2, University of Arizona, Tucson, Arizona, USA

<sup>7</sup>Honors College, University of Arizona, Tucson, Arizona, USA

<sup>8</sup>School of Natural Resources and the Environment, University of Arizona, Tucson, Arizona, USA

<sup>9</sup>Biogeochemistry Group, Department of Environmental Sciences, University of Basel, Basel, Switzerland

## Correspondence

Angelika Kübert, Ecosystem Physiology, University of Freiburg, Freiburg, Germany.  
Email: [angelika.kuebert@cep.uni-freiburg.de](mailto:angelika.kuebert@cep.uni-freiburg.de)

## Funding information

Phileology Foundation; Deutsche Forschungsgemeinschaft; European Research Council

## Abstract

The isotopic composition of xylem water ( $\delta_X$ ) is of considerable interest for plant source water studies. In-situ monitored isotopic composition of transpired water ( $\delta_T$ ) could provide a nondestructive proxy for  $\delta_X$ -values. Using flow-through leaf chambers, we monitored 2-hourly  $\delta_T$ -dynamics in two tropical plant species, one canopy-forming tree and one understory herbaceous species. In an enclosed rainforest (Biosphere 2), we observed  $\delta_T$ -dynamics in response to an experimental severe drought, followed by a  $^2\text{H}$  deep-water pulse applied belowground before starting regular rain. We also sampled branches to obtain  $\delta_X$ -values from cryogenic vacuum extraction (CVE). Daily flux-weighted  $\delta^{18}\text{O}_T$ -values were a good proxy for  $\delta^{18}\text{O}_X$ -values under well-watered and drought conditions that matched the rainforest's water source. Transpiration-derived  $\delta^{18}\text{O}_X$ -values were mostly lower than CVE-derived values. Transpiration-derived  $\delta^2\text{H}_X$ -values were relatively high compared to source water and consistently higher than CVE-derived values during drought. Tracing the  $^2\text{H}$  deep-water pulse in real-time showed distinct water uptake and transport responses: a fast and strong contribution of deep water to canopy tree transpiration contrasting with a slow and limited contribution to understory species transpiration. Thus, the in-situ transpiration method is a promising tool to capture rapid dynamics in plant water uptake and use by both woody and nonwoody species.

## KEYWORDS

CRDS, cryogenic vacuum extraction, herbaceous species, laser spectrometry, method comparison, nonwoody, woody, xylem water

## 1 | INTRODUCTION

Plants play a key role in the terrestrial water cycle, acting as an important link between soil and atmospheric water processes. Assessing and quantifying their role and functioning in ecosystem water cycling, however, remains a key challenge in ecosystem research. In particular, three fundamental aspects remain poorly understood: the quantitative contribution of plant transpiration to ecosystem evapotranspiration (ET), the use of distinct soil water sources for plant transpiration and vegetation impacts on infiltration and soil water (re)distribution (Dubbart & Werner, 2019). A central tool used to advance our understanding of these processes is the use of stable isotopic (hydrogen, H and oxygen, O) composition of water. To assess the role of plants in ecosystem water cycling, the isotopic composition of three water fluxes or pools is of particular interest: transpiration ( $\delta_T$ ), leaf water ( $\delta_L$ ) and xylem water ( $\delta_X$ ). Of these,  $\delta_X$ -values are often assumed to be isotopically representative of plant source water, as the uptake of water and transport within the plant are considered to be nonfractionating processes (e.g., Förstel, 1982; Thorburn et al., 1993; Zimmermann et al., 1968). Transpiration causes an enrichment of  $^2\text{H}$  and  $^{18}\text{O}$  in leaf water at the evaporative front and a relative depletion of these isotopes in transpired water (e.g., Dongmann et al., 1974; Ehleringer & Dawson, 1992; Flanagan et al., 1991; Förstel, 1978). Under the isotopic steady state of transpiration, the isotopic composition of water leaving the plant equals the one entering it, that is,  $\delta_T$ -values approach those of  $\delta_X$ . This state has been, for instance, observed when transpiration rates are high (Lee et al., 2007; Welp et al., 2008).

A common approach to measure  $\delta_X$ - and  $\delta_L$ -values rely on collecting (xylem/leaf) samples destructively and subsequently extracting tissue water in the laboratory by cryogenic vacuum extraction (CVE) (e.g., Ehleringer & Osmond, 1989; Ehleringer et al., 2000; Orlowski et al., 2013; West et al., 2006). However, this approach has been strongly criticized in recent years due to (1) its destructive nature and therefore limited temporal resolution, (2) its high demand in time, labour and costs and (3) its vulnerability to analytical artifacts, in particular for  $\delta^2\text{H}$ -values (e.g., Allen & Kirchner, 2021; Chen et al., 2020; Fischer et al., 2019; Kübert et al., 2020; Li et al., 2021; Orlowski et al., 2016, 2018).

To overcome these methodological concerns, research has been conducted to improve the measurements of water stable isotopes (Rothfuss & Javaux, 2017). In the last decade, laser-based techniques have been advanced to measure water stable isotopic composition directly and at high temporal resolution. These techniques have been extensively tested in the laboratory and field and frequently used to sample different ecosystem water pools, such as soil water (Kübert et al., 2020; Oerter & Bowen, 2017; Rothfuss et al., 2013; Volkmann & Weiler, 2014), transpired water (Dubbart et al., 2017; Kühnhammer et al., 2020; Simonin et al., 2013; Wang et al., 2012) and xylem water (Marshall et al., 2020; Volkmann et al., 2016). The main approach to measure  $\delta_X$ -values in-situ is by sampling the gaseous phase within trees (Marshall et al., 2020; Volkmann et al., 2016). However, this emerging approach is intrusive, restricted to larger woody species and requires

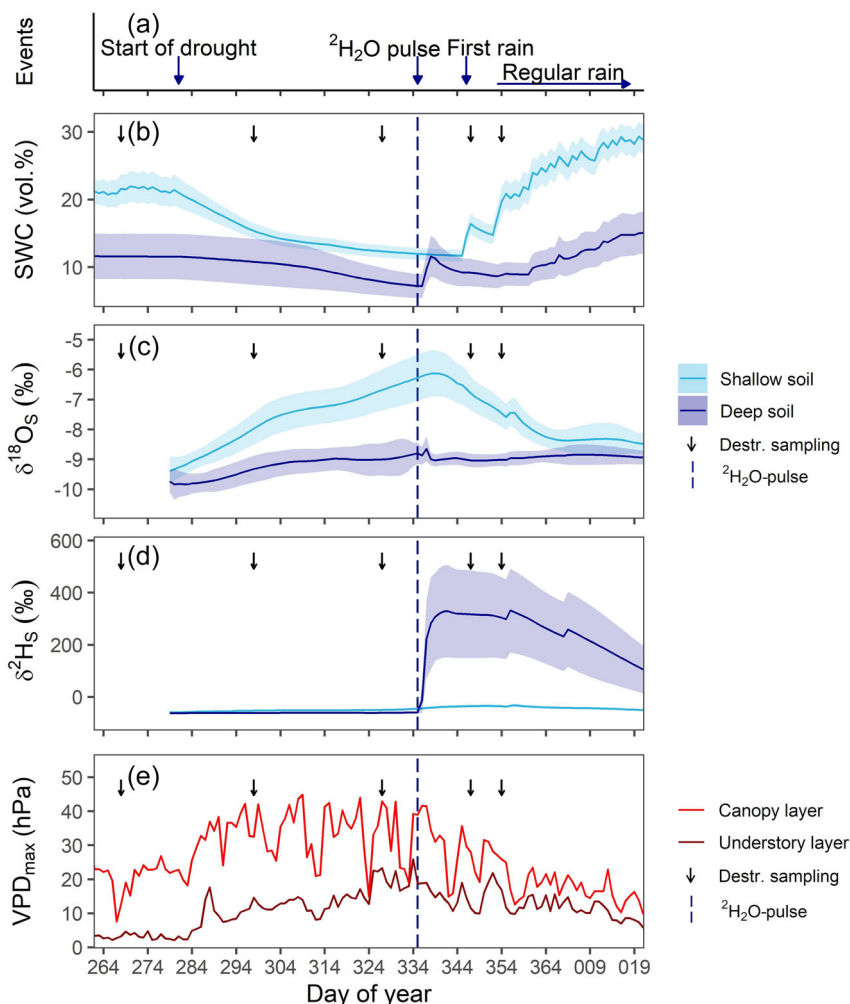
further assessment in field settings and under varying environmental conditions (see, e.g., Kühnhammer et al., 2022). An alternative approach is to derive  $\delta_X$ -values from  $\delta_L$ -values (Benettin et al., 2021; Kübert et al., 2019). This indirect estimate for  $\delta_X$ -values has been shown to be less accurate than values based on xylem sampling (Benettin et al., 2021), but has the advantage of being applicable to both woody and nonwoody plants, such as grassland species (Kübert et al., 2019).

$\delta_X$ -values, on the other hand, are also often used as a proxy for the isotopic composition of transpiration; for instance, when partitioning ET based on water stable isotopes to derive ecosystem transpiration (e.g., Williams et al., 2004; Yepez et al., 2003). This approach relies on the distinct water isotopic signatures of soil-evaporated and plant-transpired water. While soil-evaporated water gets depleted relative to soil liquid water due to isotopic fractionation, transpired water shows the isotopic signal of plant source water. The underlying assumption for this approach is that under steady-state conditions, transpired water reaches isotopic equilibrium and subsequently  $\delta_T$ -values equal those of  $\delta_X$  (Brunel et al., 1997; Chen et al., 2020; Dubbart et al., 2017; Wang et al., 2013). However, isotopic steady state might be the exception under natural conditions since  $\delta_T$ -values are strongly driven by environmental conditions and plant-specific stomatal control (Dubbart et al., 2014a, 2017; Lai et al., 2006; Simonin et al., 2013; Wang et al., 2012).  $\delta_X$ -values cannot account for nonsteady-state transpiration and  $\delta_T$ -values. Accurate  $\delta_T$ -values, though, are crucial for isotope-based ET partitioning (Dubbart et al., 2013; Rothfuss & Javaux, 2017).

Monitoring the isotopic composition of transpiration directly delivers the most accurate signal for  $\delta_T$ -values and may as well provide an accurate signal for  $\delta_X$ -values when (1) transpiration is at isotopic steady state, or (2) when integrating  $\delta_T$ -values over longer time periods (e.g., from hours to several days), assuming that isotopic nonsteady-state effects even out over time (Dubbart et al., 2014a, 2017). To derive  $\delta_T$ -values, transpired water has been sampled in several studies by enclosing leaves in bags, collecting the condensed water and subsequently measuring  $\delta_T$ -values in the laboratory. However, results have shown that this method is not reliable for the natural abundance range of water stable isotopes and requires high transpiration rates (Chakraborty et al., 2018; Kulmatiski & Forero, 2021; Menchaca et al., 2007). Chamber and cuvette techniques that directly measure the (bulk) transpiration flux, on the other hand, have been well established for decades (e.g., von Caemmerer & Farquhar, 1981; Wong, 1979) and have been applied under controlled laboratory conditions (Dubbart et al., 2017; Kühnhammer et al., 2020; Simonin et al., 2013; Wang et al., 2012). However, longer-term high-temporal resolution studies of different species conducted under varying environmental conditions, such as well-watered versus drought conditions and subsequent recovery, are still lacking.

As part of a long-term drought experiment in a model tropical rainforest (Biosphere 2) (Werner et al., 2021), we monitored  $\delta_T$ -values of two tropical plant species at the high temporal resolution, one understory herbaceous species (*Piper* sp., tentatively identified as *Piper auritum* Kunth) and one canopy-forming tree species (*Clitoria fairchildiana* R. A. Howard). We observed their response to increasing

**FIGURE 1** (a) Main hydrological events during the experiment. (b) Average soil water content (SWC, vol.%) in the shallow soil (light blue,  $\leq 50$  cm depth) and deep soil (dark blue,  $\geq 100$  cm depth), mean  $\pm$  SE. (c) Average soil water oxygen isotopic composition ( $\delta^{18}\text{O}_s$ , ‰<sub>VSMOW</sub>) in the shallow soil (light blue,  $\leq 50$  cm depth) and deep soil (dark blue,  $\geq 100$  cm depth), mean  $\pm$  SE. (d) Average soil water hydrogen isotopic composition ( $\delta^2\text{H}_s$ , ‰<sub>VSMOW</sub>) in the shallow soil (light blue,  $\leq 50$  cm depth) and deep soil (dark blue,  $\geq 100$  cm depth), mean  $\pm$  SE. (e) Maximum water vapour pressure deficit ( $\text{VPD}_{\text{max}}$ , hPa) in the canopy layer (light red,  $>7$  m) and understory layer (dark red,  $\leq 7$  m). Black arrows indicate the times of destructive sampling for xylem water, and the blue dashed line is the deep  $^2\text{H}_2\text{O}$ -pulse that was added to the bottom soil layers. VSMOW, Vienna Standard Mean Ocean Water.



drought and subsequent recovery to assess the following questions: (1) Do  $\delta_T$ -values of the studied species change over time in response to a severe drought? (2) Do  $\delta_T$ -values approach  $\delta_X$ -values and if so, when? And (3) are  $\delta_T$ -values and their relationship to  $\delta_X$ -values species-specific and affected by environmental changes?

To answer these questions, we enclosed leaves of both species in flow-through leaf chambers connected to a water isotope analyser and measured  $\delta_T$ -values 2-hourly over 5 months. Parallel to continuous measurements of  $\delta_T$ -values, branch samples were collected at five time points throughout the experiment to determine  $\delta_X$ -values from CVE. Here, we compare destructively derived  $\delta_X$ -values to  $\delta_T$ -results.

## 2 | MATERIALS AND METHODS

Water oxygen- and hydrogen-stable isotopic compositions are reported here as  $\delta$ -notation, relative to Vienna Standard Mean Ocean Water (VSMOW; Gonfiantini, 1978;  $\delta = [(R_{\text{sample}} - R_{\text{VSMOW}})/R_{\text{VSMOW}}]$ , expressed in ‰).  $\delta$  of a certain compartment/flux (written as index) represents values of both isotopes, that is,  $\delta_T$  refers to  $\delta^2\text{H}$ - and  $\delta^{18}\text{O}$ -values of  $T$ .

All results in the text are given as mean  $\pm$  standard error, unless stated otherwise. Calculations of SE included error propagation in every step of data processing (if applicable). For mixed operations, we used Monte Carlo-based error propagation (1000 iterations) to determine uncertainties (Ladd & Sachs, 2015).

### 2.1 | Experimental design

The Biosphere 2 model tropical rainforest was subjected to a long-term drought of 65 days, starting at the Day of year (DoY) 281, with subsequent recovery initiated by adding a water pulse to the deep soil layers (DoY: 335–337), a first rain event (DoY: 346) and the return to the regular rain (DoY: 351; Figure 1a; see Werner et al. (2021) for more details on experimental design). The experiment thus comprised five distinct periods, which were defined as follows: (1) predrought, DoY: 268–281, (2) mild drought, DoY: 298–308, (3) severe drought, DoY: 324–335, (4)  $^2\text{H}_2\text{O}$ -pulse, DoY: 335–345 and (5) onset of rain and early recovery, DoY: 351–361.

For the predrought and recovery phase, rainwater (typically the only source water for the model rainforest) was provided by large-volume storage tanks supplied from an on-site well and therefore had only a small variation in its isotopic composition throughout the experiment ( $\delta^2\text{H} = -62.7 \pm 0.2\text{‰}$ ,  $\delta^{18}\text{O} = -9.0 \pm 0.0\text{‰}$ ). The  $^2\text{H}_2\text{O}$ -pulse ( $\sim 23\,000\text{ L}$ ) was strongly enriched in  $^2\text{H}$  ( $\delta^2\text{H} \sim 2200\text{‰}$ ,  $\delta^{18}\text{O} = -8.8\text{‰}$ ) and added to the bottom soil layers of the model rainforest (dependent on location: 180–300 cm depth; water column: 5–7 cm).

## 2.2 | Environmental conditions

Environmental conditions in the model rainforest were monitored continuously throughout the experiment (see Werner et al., (2021). At four towers (S, NE, NW and mountain top) at several heights (1, 3, 7, 13 and [only S and NE towers] 20 m above soil surface), photosynthetic photon flux density (PPFD,  $\text{mmol m}^{-2} \text{day}^{-1}$ ; Apogee SQ110; Campbell Scientific), air temperature ( $T_{\text{air}}$ ,  $^{\circ}\text{C}$ ) and air relative humidity (RH, %) (Vaisala HMP 45c; Vaisala Oyj) were measured every minute and logged as 15-min averages. Sensors for  $T_{\text{air}}$  and RH were protected by radiation shields (41003-5; Campbell Scientific). Water vapour pressure deficit (VPD, hPa) was calculated from  $T_{\text{air}}$  and RH after Tetens (1930). The VPD in the canopy layer was derived as average from the heights  $>7\text{ m}$ , and the VPD of the understory layer was based on the average of the heights  $\leq 7\text{ m}$  (see Werner et al. (2021) for more details).

Soil water content (SWC, vol.%, SMT100; Truebner GmbH), soil temperature ( $T_{\text{soil}}$ ,  $^{\circ}\text{C}$ ; SMT100, Truebner GmbH) and soil water isotopic composition ( $\delta_{\text{S}}$ ,  $\text{‰}_{\text{VSMOW}}$ ) were monitored in four soil pits (P) located across the model rainforest (NE, NW, SE and central, referred to as P1, P2, P3 and P4). SWC-,  $T_{\text{soil}}$ - and  $\delta_{\text{S}}$ -values were measured at 5, 10, 20, 50 and 100 cm depth in each pit, and depending on the pit's depth, at 200 cm and maximum depth (max. depth: P1: 180, P2: 310, P3: 290 and P4: 200 cm depth). Data were logged every 15 min using SDI-12 protocols on separate CR1000 dataloggers (Campbell Scientific). SWC and  $T_{\text{soil}}$  were gap filled by correlation with the nearest working sensors, either by height or within the profile. SWC of shallow soil was calculated as the average of all sensors at soil depths  $\leq 50\text{ cm}$ , and SWC of deep soil as the average at soil depths  $\geq 100\text{ cm}$ .

$\delta_{\text{S}}$ -values were derived in-situ by sampling the water vapour intruding into a piece of gas-permeable (GP) microporous polypropylene tubing (Accurel GP V8/2HF, 3M; 0.155 cm wall thickness, 0.55 cm i.d., 0.86 cm o.d.) assuming direct water vapour equilibration (as in Rothfuss et al., 2013; Volkmann & Weiler, 2014). The isotopic composition of soil water vapour diffusing into the GP tubes was measured by a water isotope analyser (L2130i; Picarro Inc.), with only the L2130i pump pulling on the GP tubes ( $\sim 30\text{ ml min}^{-1}$ ). Automatic switching between measurements (i.e., between soil pits and soil depths) was done via a manifold (16-Port Distribution Manifold; A0311; Picarro Inc.), sampling GP tubes for 20–30 min to reach a stable plateau of the isotopic composition of the sampled soil water vapour ( $\delta_{\text{V}}$ ) and water mixing ratios (MRs). The selection of steady  $\delta_{\text{V}}$ - and MR-values was based on moving averages of

the coefficients of variation (for more details see Kübert et al., 2020).  $\delta_{\text{S}}$ -values were then derived from  $\delta_{\text{V}}$ -values under the assumption of isotopic thermodynamic equilibrium, using  $T_{\text{soil}}$  of the respective soil depth for conversion (Majoube, 1971; Horita & Wesolowski, 1994).

The water isotope analyser was calibrated during the experiment by measuring three laboratory water isotope standards ( $\delta^2\text{H}$ :  $-140.30\text{‰}$ ,  $+25.04\text{‰}$  and  $+454.58\text{‰}$ ;  $\delta^{18}\text{O}$ :  $-19.16\text{‰}$ ,  $-6.66\text{‰}$  and  $+5.29\text{‰}$ ) each night at different water MRs (range: 0– $\sim 25\,000\text{ ppm}$ ). All laboratory isotope standards were calibrated against international isotope standards: VSMOW, SLAP and GISP (IAEA). Variation of water vapour mixing ratios of measurements was relatively small ( $27\,729 \pm 3087\text{ ppm}$ , mean  $\pm$  SD), and therefore no correction for concentration dependency was applied to isotopic measurements. Mean measurement precision was  $\pm 0.17\text{‰}$  for  $\delta^{18}\text{O}$  and  $\pm 0.54\text{‰}$  for  $\delta^2\text{H}$  ( $\pm$ SD, comparison of repeated standard measurements over the entire experiment phase). Smoothing functions of derived  $\delta_{\text{S}}$ -values were calculated for each soil pit and depth using locally estimated scatterplot smoothing (predict function, R version 3.6.0). In case of 2-cm soil depth and the maximum depths of each pit (where the  $^2\text{H}$ -labelled water was added), the data set was split into two parts (2-cm depth: before and after first rain; maximum depths: before and after  $^2\text{H}_2\text{O}$ -pulse) for smoothing to account for fast changes in  $\delta_{\text{S}}$ -values. For P1 and P3, the transit period (DoY: 336–338 and DoY: 339, respectively) was linearly interpolated. No data were available from January 3 18:00 to January 17 18:00 due to condensation.  $\delta_{\text{S}}$ -values of shallow soil were calculated as the average of smoothed curves at soil depths  $\leq 50\text{ cm}$ , and  $\delta_{\text{S}}$ -values of deep soil as the average at soil depths  $\geq 100\text{ cm}$ .

## 2.3 | In-situ transpiration and stomatal conductance

Leaf transpiration of two species, the understory herbaceous species *P. auritum* L. ( $n=4$ ) and the canopy tree species *C. fairchildiana* R. A. Howard ( $n=3$ ), was monitored throughout the experiment. To monitor leaf transpiration, leaves were enclosed in self-made flow-through leaf chambers constructed from fluorinated ethylene propylene film (85905K64; McMaster Carr) and equipped with a fan to ensure effective air mixing (MC25101V2; Sunon). One chamber was left empty (=blank chamber) to sample the air entering the leaf chambers. All chambers were continuously flushed with an air mixture ( $1\text{ L min}^{-1}$ ) providing a controlled amount of  $\text{CO}_2$  ( $\sim 500\text{ ppm}$ ) and water vapour ( $\sim 3000\text{ ppm}$ ). Flushing and ventilation of leaf chambers were important to avoid overheating. Leaf temperature ( $^{\circ}\text{C}$ ) and PPFD ( $\mu\text{mol m}^{-2} \text{s}^{-1}$ ) were monitored for each leaf by a self-made, battery-powered logger system. The outlets of leaf chambers (=exiting air stream) and the blank chamber (=entering air stream) were sampled by a water isotope analyser (Picarro L2120i; Picarro Inc.) for 5 min each, using a distribution manifold system (custom aluminium blocks with ports) connected to a pump (KNF). All tubing was made of perfluoroalkoxy alkanes (Ametek) and heated to avoid

condensation and consequential isotopic fractionation. For analysis, 2-min averages (2.5–4.5 min) of water mixing ratios and respective isotopic compositions were computed from the 5-min intervals.

The isotopic composition of transpired water ( $\delta_T$ ) was determined by mass balance (Dubbett et al., 2014a, 2017; Simonin et al., 2013), comparing the air streams entering (in; i) and exiting (out; o) the leaf chambers (Equation 1):

$$\delta_T = \frac{\delta_o W_o - \delta_i W_i - W_o W_i (\delta_o - \delta_i)}{W_o - W_i} \quad (1)$$

The gas exchange parameters transpiration ( $T$ ,  $\text{mmol m}^{-2} \text{s}^{-1}$ ) and stomatal conductance ( $g_s$ ,  $\text{mmol m}^{-2} \text{s}^{-1}$ ) were calculated after von Caemmerer and Farquhar (1981).  $\delta_T$ ,  $T$ - and  $g_s$ -values of dying leaves were excluded from the analysis (Supporting Information: Table S1 for data input). Data gaps of  $\leq 4$  h were filled by linear interpolation, and data gaps of  $>4$  but  $<24$  h were filled by averaging values of the same time period on the day before and after the data gap (only of  $T$  and  $g_s$ , more information see Werner et al., 2021).

The water isotope analyser was calibrated in the laboratory against four laboratory water isotope standards spanning a wide isotopic range ( $\delta^2\text{H}$ :  $-102.90\text{‰}$ ,  $-64.01\text{‰}$ ,  $-10.27\text{‰}$  and  $53.89\text{‰}$ ;  $\delta^{18}\text{O}$ :  $-25.13\text{‰}$ ,  $-9.28\text{‰}$ ,  $-5.22\text{‰}$  and  $-0.40\text{‰}$ ) and water mixing ratio range ( $\sim 2500$ – $\sim 40\,000$  and  $\sim 5000$  ppm steps) and corrected for mixing ratio dependency (Schmidt et al., 2010). Mean measurement precision was  $\pm 0.05\text{‰}$  for  $\delta^{18}\text{O}$  and  $\pm 0.21\text{‰}$  for  $\delta^2\text{H}$  ( $\pm\text{SD}$ ). To account for drifts, parallel measurements of the atmospheric water vapour, made by the L2120i and another water isotope laser (TILDAS; Aerodyne), were used as a cross-calibration. All laboratory isotope standards were calibrated against international isotope standards: VSMOW, SLAP and GISP (IAEA).

## 2.4 | Destructive xylem sampling and CVE

Xylem tissue of the two species (*P. auritum* L.:  $n = 4$ ; *C. fairchildiana*:  $n = 3$ ) was sampled at five discrete time points throughout the experiment (predrought, DoY: 268; mild drought, DoY: 298; severe drought, DoY: 327;  $^2\text{H}_2\text{O}$ -pulse, DoY: 347; onset of regular rain, DoY: 354). Branches in the crown of the plant individuals were cut, bark and phloem removed and samples immediately frozen until water extraction. Samples were extracted by CVE, that is, by heating to  $\sim 95^\circ\text{C}$  for 120 min under vacuum of 0.1 mbar (XDS10 vacuum pump; Edwards) and water vapour was trapped in liquid  $\text{N}_2$  traps (custom-built vacuum line, similar to Ehleringer & Dawson (1992); design of R. Siegwolf). Extracted water was then filtered to remove potential organic compounds (glass fibre, retention capacity 1–2 mm, KC98.1; Roth). After filtration, liquid water samples were stored in threaded glass vials (ND9; LLG) with closed lids at  $4^\circ\text{C}$  until isotopic analysis. Isotopic analysis was conducted with an A0325 robotic autosampler delivering water samples to a V1102-i vaporization module coupled to a water isotope analyser (L2130i; all Picarro Inc.). Extracted water samples were calibrated against four laboratory isotope standards

( $\delta^2\text{H}$ :  $-102.90\text{‰}$ ,  $-64.01\text{‰}$ ,  $-10.27\text{‰}$  and  $53.89\text{‰}$ ;  $\delta^{18}\text{O}$ :  $-25.13\text{‰}$ ,  $-9.28\text{‰}$ ,  $-5.22\text{‰}$  and  $-0.40\text{‰}$ ) referenced to international isotope standards: VSMOW, SLAP and GISP (IAEA). Mean measurement precision was  $\pm 0.06\text{‰}$  for  $\delta^{18}\text{O}$  and  $\pm 0.17\text{‰}$  for  $\delta^2\text{H}$  ( $\pm\text{SD}$ ). Obtained results of extracted water samples were postprocessed with ChemCorrectTM (Picarro Inc.) to detect possible organic contamination. Three of the 35 analysed samples did not yield sufficient water for isotopic analysis (all *P. auritum*; DoY: 268, 347 and 354), 3 were flagged red ('substantial contamination') by the software and 12 were flagged yellow ('some contamination'). None of the contaminated samples were excluded due to a minor impact on isotopic composition (Supporting Information: Figure S1).

## 2.5 | Analysis of $\delta_T$ and comparison of methods

Several approaches were tested to derive  $\delta_X$ -values from in-situ isotopic measurements (InS) of transpiration (referred to as  $\delta_{\text{InS}}$ ): (1) daily mean of  $\delta_T$ -values, (2) daytime mean of  $\delta_T$ -values and (3)  $\delta_T$ -values during midday when  $T$  was the highest. Daytime was defined as PPDF in the model rainforest  $>10 \mu\text{mol m}^{-2} \text{s}^{-1}$  and midday as  $>9:30$  and  $<15:30$ .

Moreover, the same approaches were used but accounting for the mass flux of transpiration, that is, weighted by the flux  $T$  using Equation (2):

$$\delta_{\text{InS (flux-weighted)}} = \frac{\sum_{z=1}^n (T_z * \delta_{T_z})}{\sum_{z=1}^n T_z} \quad (2)$$

$T_z$  and  $\delta_{T_z}$  are  $T$ - and  $\delta_T$ -values at the time point  $z$ .  $n$  is the number of measurement values during the respective time period (i.e., daily, daytime and midday). The product of  $T_z$  and  $\delta_{T_z}$ -values is also called the isoflux of transpiration.

This resulted in (4) flux-weighted daily mean of  $\delta_T$ -values, (5) flux-weighted daytime mean of  $\delta_T$ -values and (6) flux-weighted  $\delta_T$ -values during midday when  $T$  was the highest. Approaches 1–3 are later referred to as 'simple mean approaches', and 4–6 as 'flux-weighted mean approaches'. Furthermore, moving averages of  $\delta_T$ -values (2–5 days) were calculated to assess the impact of the nonsteady state of transpiration since nonsteady-state conditions can prevail for days (Dubbett et al., 2014a).

$\delta_X$ -values derived from destructive sampling and CVE were compared to 3-day averages (day of sampling  $\pm 1$  day) of  $\delta_T$ -values to account for possible nonsteady-state effects of transpiration (species mean in each case). Mean absolute differences ( $\Delta$ ) were calculated as the difference between CVE and in-situ isotopic measurements (InS) of transpiration. Since the automated leaf chamber measurements started on DoY 277, the destructive sampling of DoY 268 was compared to DoY 277–279 of in-situ transpiration measurements.

## 2.6 | Statistical analysis

We performed linear mixed-effect models to test the effect of  $g_s$  and  $T$  on variations of  $\delta_T$ -values and to assess statistical differences



between methods (CVE and in-situ transpiration), approaches of in-situ transpiration and species. Moreover, we tested the effect of drought on the agreement of CVE- and transpiration-derived  $\delta_x$ -values. We added DoY and plant individuals as random factors to account for repeated measurements. In case of  $\delta^2\text{H}$ , the  $^2\text{H}_2\text{O}$ -pulse phase was excluded from statistical analysis due to the high isotopic variation introduced by the  $^2\text{H}_2\text{O}$ -pulse. All analyses were conducted in R (version 4.1.2; R Foundation for Statistical Computing). Additional software packages used for models were lme4 (Bates et al., 2015) and lmerTest (Kuznetsova et al., 2020).

### 3 | RESULTS

#### 3.1 | Environmental conditions in the model rainforest

Drought led to a decrease in SWC, in both shallow and deep soil layers. Under predrought conditions, the mean SWC of shallow and deep soil was 23 and 12 vol.%, respectively (Figure 1b). After drought was induced, shallow soil layers immediately dried down and dropped below 15 vol.% after 19 days, while deep soil layers showed a steep decrease ( $>1$  vol.% per day) later during the drought (from DoY 311 on) and dropped below 10 vol.% after 29 days of drought. The  $^2\text{H}_2\text{O}$ -pulse was clearly visible in the deep soil layers. After the onset of rain, both shallow and deep soil layers returned to and even exceeded predrought values of SWC (28 and 14 vol.%, respectively, DoY: 10–19).

Soil drying and related evaporation led to an increase in  $\delta_s$ -values, which was visible in both shallow and deep soil layers. Before the drought, the mean  $\delta^{18}\text{O}_s$  and  $\delta^2\text{H}_s$  of shallow soil were  $-9.4 \pm 0.7\text{‰}$  and  $-59.3 \pm 6.6\text{‰}$ , respectively, and mean  $\delta^{18}\text{O}_s$  and  $\delta^2\text{H}_s$  of deep soil were  $-9.8 \pm 0.5$  and  $-63.1 \pm 2.8\text{‰}$ , respectively (Figure 1c,d). While  $\delta_s$ -values of shallow soil layers increased quickly and steadily during drought (increase to  $-6.1\text{‰}/-36.3\text{‰}$  for  $\delta^{18}\text{O}_s/\delta^2\text{H}_s$ ), deep soil layers had only a small increase in  $\delta^{18}\text{O}_s$  and  $\delta^2\text{H}_s$  (increase to  $-8.8\text{‰}$  and  $-59.8\text{‰}$ , respectively,  $^2\text{H}_2\text{O}$ -pulse phase excluded). In particular, in the upper 2 cm, we observed a strong increase from  $-8.3\text{‰}$  to  $-0.3\text{‰}$  ( $\delta^{18}\text{O}_s$ ) and  $-55.7\text{‰}$  to  $-18.6\text{‰}$  ( $\delta^2\text{H}_s$ ;  $^2\text{H}_2\text{O}$ -pulse phase excluded, data not shown).

The  $^2\text{H}_2\text{O}$ -pulse was clearly visible in the deep soil layers, with  $\delta^2\text{H}_s$ -values increasing from  $-59.8\text{‰}$  to  $+327.7\text{‰}$ . After the onset of rain, shallow soil layers approached predrought values of  $\delta^2\text{H}_s$  and  $\delta^{18}\text{O}_s$  ( $-48.9\text{‰}$  and  $-8.4\text{‰}$ , respectively, DoY: 17–20). In addition,  $\delta^2\text{H}_s$  of deep soil decreased steadily, indicating drainage, use and dilution of the added  $^2\text{H}_2\text{O}$ -pulse ( $\delta^2\text{H}_s$ :  $+127.5\text{‰}$ ;  $\delta^{18}\text{O}_s$ :  $-8.9\text{‰}$ ).

Maximum VPD ( $\text{VPD}_{\text{max}}$ ) clearly differed for canopy and understory vegetation layers (Figure 1e). With the onset of drought,  $\text{VPD}_{\text{max}}$  of both layers increased (canopy:  $+10$  hPa; understory:  $+27$  hPa; predrought to severe drought). Accordingly, VPD in the leaf chambers increased as well, though, the increase in VPD was stronger for the understory species *P. auritum* (Supporting Information: Figure S2).

#### 3.2 | Response to drought and rewetting: $T$ , $g_s$ and $\delta_T$ from in-situ measurements

In response to the soil water deficit, both plant species strongly reduced  $T$  and  $g_s$  (Figure 2a,b). The response in  $g_s$  was, however, more pronounced for *P. auritum*. For *C. fairchildiana*,  $T$  and  $g_s$  decreased by 56% and 58% respectively. For *P. auritum*, they dropped by 65% and 95% from predrought to severe drought. Generally, *P. auritum* had higher  $g_s$ -values, likely related to the lower VPD in the understory layer (Supporting Information: Figure S2). After the  $^2\text{H}_2\text{O}$ -pulse, we observed a small recovery for both species in  $T$  and  $g_s$ . The strong recovery, though, occurred only after the onset of regular rain.

$\delta^{18}\text{O}_T$  and  $\delta^2\text{H}_T$ -values of *P. auritum* were generally higher than those of *C. fairchildiana* throughout the experiment ( $p < 0.05$  and  $p < 0.01$ ; Figure 2c,d). In response to soil drying and increasing VPD,  $\delta^{18}\text{O}_T$ -values (Figure 2c) increased markedly for *P. auritum* (from  $-10.6\text{‰}$  to  $-0.2\text{‰}$  in 53 days). A slight increase was also observed for  $\delta^{18}\text{O}_T$  of *C. fairchildiana* (from  $-12.4\text{‰}$  to  $-6.5\text{‰}$ ). After the  $^2\text{H}_2\text{O}$ -pulse and onset of rain,  $\delta^{18}\text{O}_T$ -values of both *C. fairchildiana* and *P. auritum* decreased to values of the predrought phase.  $\delta^{18}\text{O}_T$ -values of *P. auritum*, however, had not completely returned to predrought values by DoY 19 ( $-6.8\text{‰}$ ).

$\delta^2\text{H}_T$ -values displayed a similar pattern as  $\delta^{18}\text{O}_T$ -values before the  $^2\text{H}_2\text{O}$ -pulse. One day after the  $^2\text{H}_2\text{O}$ -pulse,  $\delta^2\text{H}_T$ -values of *C. fairchildiana* were increasing rapidly by  $\sim +20.7\text{‰}$  per day, which confirms that these trees had access to deep soil water (Figure 2d).  $\delta^2\text{H}_T$ -values of *P. auritum* also increased, but the response occurred 10 days later and was less pronounced ( $+5.1\text{‰}$  per day).

We observed strong variation in the diurnal course of  $\delta_T$ -values for *C. fairchildiana* in the predrought and recovery phase (Figure 3a,c,e). During predrought and recovery,  $\delta_T$ -values of both species were generally higher during midday and lower at other times of the day. The amplitude of the diurnal variation strongly declined with increasing drought. While under predrought conditions, the amplitude of  $\delta^{18}\text{O}_T$  and  $\delta^2\text{H}_T$ -values was up to  $\sim 5.3\text{‰}$  and  $41.7\text{‰}$  (*C. fairchildiana*) and  $\sim 2.9\text{‰}$  and  $8.0\text{‰}$  (*P. auritum*), respectively, it declined to  $\sim 4.1\text{‰}$  and  $11.3\text{‰}$  for *C. fairchildiana* and remained similar with  $\sim 3.0\text{‰}$  and  $8.8\text{‰}$  for *P. auritum*. During recovery, the amplitude of the diurnal variation was partly even more pronounced:  $\sim 8.8\text{‰}$  and  $33.0\text{‰}$  (*C. fairchildiana*) and  $\sim 3.9\text{‰}$  and  $12.8\text{‰}$  (*P. auritum*), additionally amplified by the  $^2\text{H}_2\text{O}$ -pulse.

Diurnal variation of  $\delta_T$ -values was closely linked to diurnal variation in stomatal conductance. Accordingly,  $\delta_T$ - and  $g_s$ -values of both species were the highest during midday, and the amplitudes of diurnal  $g_s$  variation decreased with increasing drought and increased again during recovery (Figure 3g–i). Under predrought conditions, the amplitude of  $g_s$  was up to 93 (*C. fairchildiana*) and 158  $\text{mmol m}^{-2} \text{s}^{-1}$  (*P. auritum*). It declined to 15 (*C. fairchildiana*) and 8  $\text{mmol m}^{-2} \text{s}^{-1}$  (*P. auritum*) during severe drought. During recovery, the amplitude of the diurnal  $g_s$  variation was even higher than under predrought conditions for *C. fairchildiana* (253  $\text{mmol m}^{-2} \text{s}^{-1}$ , Figure 3k). Lower  $g_s$  during drought led to higher  $\delta^{18}\text{O}$  fractionation (i.e., lower  $\delta^{18}\text{O}_T$ -values), higher  $g_s$  during predrought and recovery led to less fractionation (i.e., higher  $\delta^{18}\text{O}_T$ -values) during midday (Figure 3a,b).

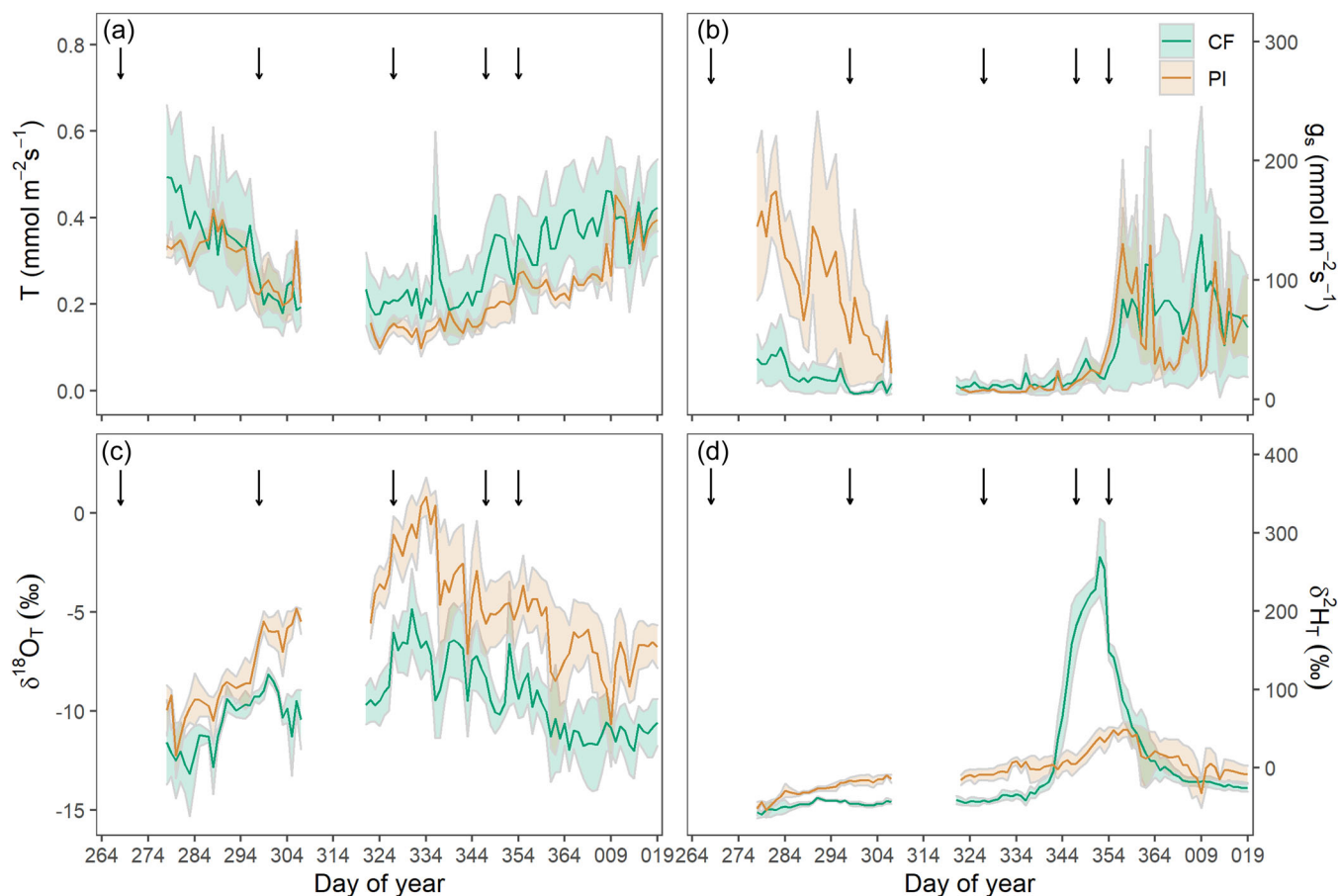


**FIGURE 2** (a) Transpiration ( $T$ ,  $\text{mmol m}^{-2} \text{s}^{-1}$ ), (b) stomatal conductance ( $g_s$ ,  $\text{mmol m}^{-2} \text{s}^{-1}$ ), (c) oxygen isotopic composition of transpired water ( $\delta^{18}\text{O}_T$ , ‰<sub>VSMOW</sub>) and (d) hydrogen isotopic composition of transpired water ( $\delta^2\text{H}_T$ , ‰<sub>VSMOW</sub>) during drought and rewetting for *Clitoria fairchildiana* (CF, green) and *Piper auritum* (PI, brown). Mean  $\pm$  SE. Black arrows indicate the times of destructive sampling for xylem water and the blue dashed line the  $^2\text{H}_2\text{O}$ -pulse. VSMOW, Vienna Standard Mean Ocean Water. [Color figure can be viewed at [wileyonlinelibrary.com](https://onlinelibrary.wiley.com/doi/10.1111/pce.14475)]

Amplitudes of  $\delta_T$ -values were positively correlated to amplitudes of  $g_s$  for both species in the case of  $\delta^{18}\text{O}_T$  (*C. fairchildiana*:  $p < 0.001$ ; *P. auritum*:  $p < 0.1$ ). For  $\delta^2\text{H}_T$ , this was only true for *C. fairchildiana* ( $p < 0.001$ ; *P. auritum*:  $p = 0.3$ ). A significant impact of  $g_s$  was found for both species on  $\delta^{18}\text{O}_T$ -values ( $p < 0.001$ ) but only for *P. auritum* on  $\delta^2\text{H}_T$ -values ( $p < 0.01$ ; *P. auritum*:  $p = 0.6$ ).

### 3.3 | Response to drought and rewetting: $\Delta_x$ from CVE

Generally,  $\delta_x$ -values derived from CVE (referred to as  $\delta_{\text{CVE}}$ ) of both species were highly variable (Figure 4). Moreover,  $\delta_{\text{CVE}}$ -values of *P. auritum* were generally higher than  $\delta_{\text{CVE}}$ -values of *C. fairchildiana* ( $p < 0.001$ ) throughout the experiment (in line with observed  $\delta_T$ -values; Figure 2c,d).  $\delta^{18}\text{O}_{\text{CVE}}$ -values (Figure 4a,b) increased slightly for both *C. fairchildiana* and *P. auritum* in response to drought, which was more pronounced for *P. auritum* (*P. auritum*: from  $-4.8\%$  to  $-2.5\%$ ; *C. fairchildiana*: from  $-6.1\%$  to  $-5.7\%$ ; predrought vs. severe drought).  $\delta^2\text{H}_{\text{CVE}}$  values had a similar pattern as  $\delta^{18}\text{O}_{\text{CVE}}$ -values before the  $^2\text{H}_2\text{O}$ -pulse (Figure 4c-e; *P. auritum*: from  $-44.3\%$  to

$-37.0\%$ ; *C. fairchildiana*: from  $-56.4\%$  to  $-56.5\%$ ). The variation of  $\delta^2\text{H}_{\text{CVE}}$ -values among and within species was higher after the  $^2\text{H}_2\text{O}$ -pulse.  $\delta^2\text{H}_{\text{CVE}}$ -values of *C. fairchildiana* increased considerably (from  $-56.5\%$  up to  $+381.9\%$ ), confirming access to water in the deepest soil layers, as seen in transpiration  $\delta^2\text{H}$ -values (Figure 2d).  $\delta^2\text{H}_{\text{CVE}}$ -values of *P. auritum* also increased, but the response was less pronounced (from  $-37.0\%$  to  $+67.9\%$ ), indicating a lower contribution of deep soil water to  $T$ .

### 3.4 | Analysis of $\delta_T$ and comparison of methods

To derive  $\delta_x$ -values from in-situ isotopic measurements of transpiration ( $\delta_{\text{ins}}$ ), we used six different approaches, that is, the simple mean and flux-weighted mean of daily, daytime and midday  $\delta_T$ -values (Figures 5 and 6 Supporting Information: Figure S3). Differences in  $\delta_{\text{ins}}$  were small and nonsignificant between different averaging periods (i.e., daily, daytime and midday) periods, for both simple mean and flux-weighted mean approaches (Table 1). The flux-weighted mean approaches generally showed a slightly better agreement with CVE-derived  $\delta_x$ -values than the

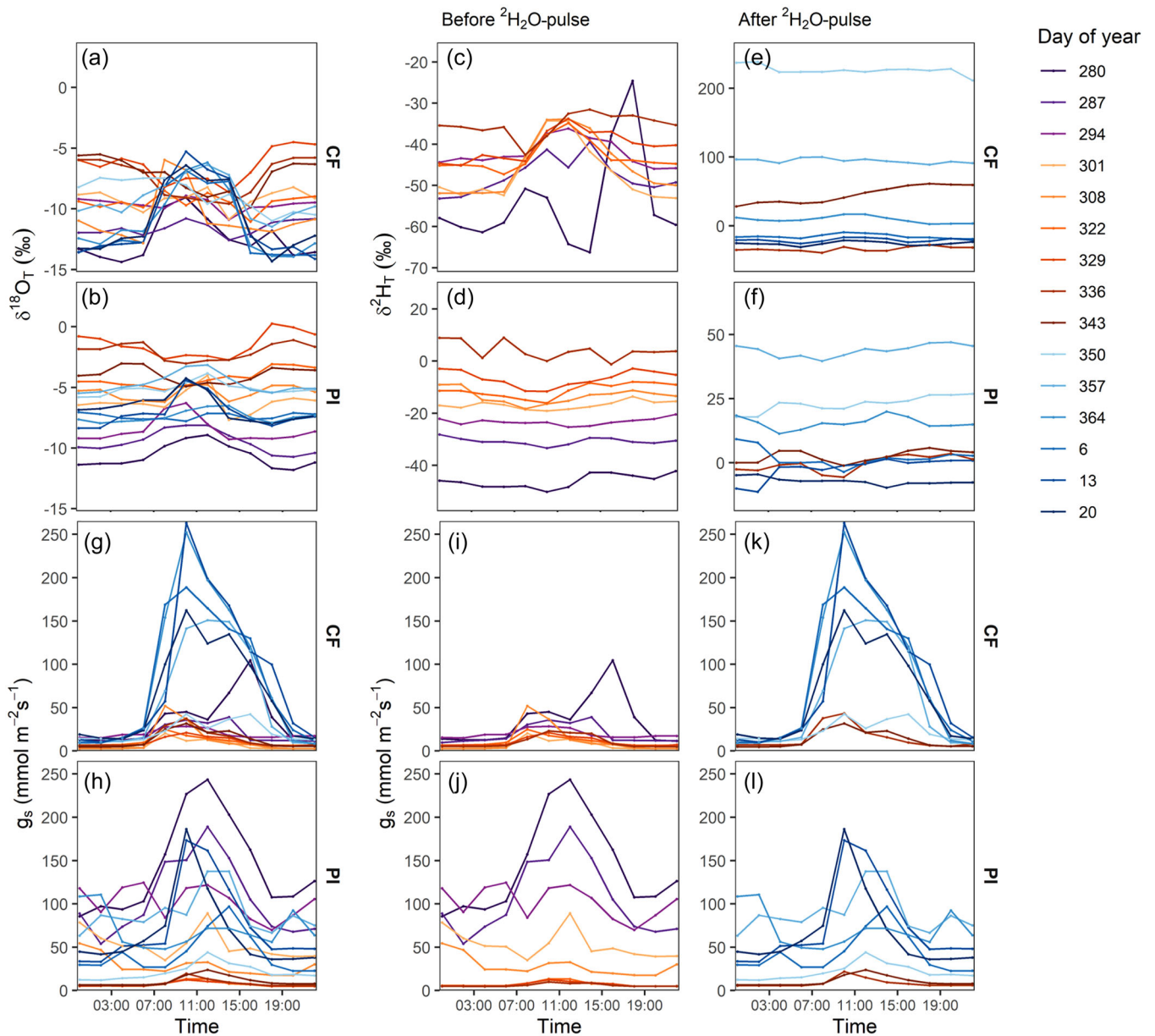


**FIGURE 3** Mean diurnal courses of the isotopic composition of transpired water ( $\delta_T$ , a–f) and stomatal conductance ( $g_s$ ,  $\text{mmol m}^{-2} \text{s}^{-1} \text{g}^{-1}$ ) in 7-day averaged intervals (labelled by Day of year [DoY] midpoint). Oxygen isotopic composition of transpired water ( $\delta^{18}\text{O}_T$ , ‰<sub>VSMOW</sub>) of *Clitoria fairchildiana* (a) and *Piper auritum* (b). Hydrogen isotopic composition of transpired water ( $\delta^2\text{H}_T$ , ‰<sub>VSMOW</sub>) of *C. fairchildiana* (c) and *P. auritum* (c) before the  $^2\text{H}_2\text{O}$ -pulse, and *C. fairchildiana* (e) and *P. auritum* (f) after the  $^2\text{H}_2\text{O}$ -pulse.  $g_s$  of *C. fairchildiana* (g) and *P. auritum* (h).  $g_s$  of *C. fairchildiana* (i) and *P. auritum* (j) before the  $^2\text{H}_2\text{O}$ -pulse, and *C. fairchildiana* (k) and *P. auritum* (l) after the  $^2\text{H}_2\text{O}$ -pulse. Violet colours indicate predrought, red colours drought and blue colours after-drought conditions. Note the different scale for (c)–(f). CF, *C. fairchildiana*; PI, *P. auritum*; VSMOW, Vienna Standard Mean Ocean Water. [Color figure can be viewed at [wileyonlinelibrary.com](https://onlinelibrary.wiley.com/doi/10.1111/pce.14475)]

simple mean approaches for  $\delta^{18}\text{O}$  (mean absolute difference: 3.1‰ and 3.2‰, respectively), likely because they account for the mass flux of transpiration. Moreover, differences between daily, daytime and midday values were small (4.1‰, 4.1‰ and 4.0‰, respectively; flux-weighted mean).  $\delta^{18}\text{O}_{\text{CVE}}$ -values of *C. fairchildiana* were consistently higher than  $\delta^{18}\text{O}_{\text{INS}}$ -values ( $p < 0.001$ ), differences ranging from +1.7‰ to +5.9‰. Differences for *P. auritum* ranged from −0.5‰ to +6.2‰, and CVE- and transpiration-derived values partly matched.

For  $\delta^2\text{H}$  (Figure 6), simple mean approaches showed a better agreement with CVE-derived  $\delta_X$ -values than the flux-weighted mean approaches (−10.4‰ and −10.8‰, respectively). Predrought  $\delta^2\text{H}_{\text{INS}}$ -values were not significantly different from  $\delta^2\text{H}_{\text{CVE}}$ -values for all approaches and both species. During drought,  $\delta^2\text{H}_{\text{INS}}$  were consistently higher than  $\delta^2\text{H}_{\text{CVE}}$ -values for all approaches and both species, with differences ranging from −28.2‰ to −3.8‰.

For  $\delta^{18}\text{O}$ , the agreement of transpiration- and CVE-derived values was higher for *P. auritum*. For  $\delta^2\text{H}$ , derived values of



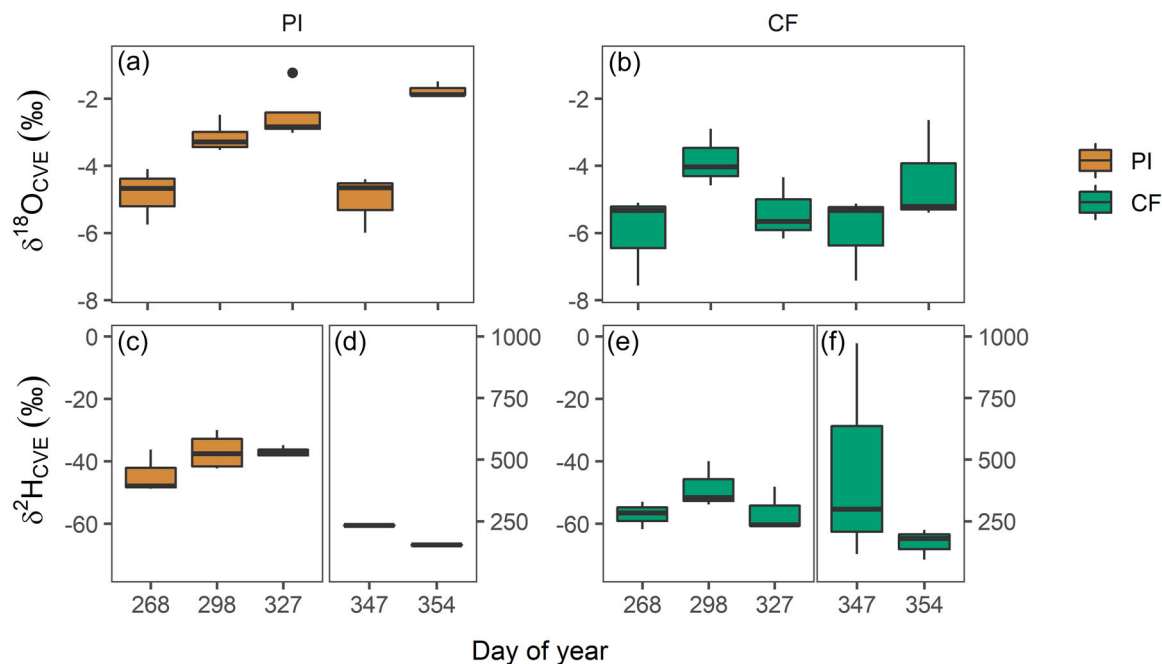


**FIGURE 4** Xylem water isotopic composition derived from cryogenic vacuum extraction ( $\delta_{\text{CVE}}$ ) during drought and recovery. Oxygen isotopic composition ( $\delta^{18}\text{O}_{\text{CVE}}$ , ‰<sub>VSMOW</sub>) for (a) *Piper auritum* (PI, brown) and (b) *Clitoria fairchildiana* (CF, green). Hydrogen isotopic composition ( $\delta^2\text{H}_{\text{CVE}}$ , ‰<sub>VSMOW</sub>) for *P. auritum* (PI, brown) before (c) and after (d) the  $^2\text{H}_2\text{O}$ -pulse and *C. fairchildiana* (CF, green) before (e) and after (f) the  $^2\text{H}_2\text{O}$ -pulse. Boxplot of the median (solid black line), upper and lower quartiles (box), 1.5 interquartile range (whiskers) and outliers (circles). Note the different scale of (c)–(f). VSMOW, Vienna Standard Mean Ocean Water. [Color figure can be viewed at [wileyonlinelibrary.com](https://onlinelibrary.wiley.com/doi/10.1111/pce.14475)]

*C. fairchildiana* matched better (all six approaches; Table 1). While the agreement of transpiration- and CVE-derived values increased during drought for  $\delta^{18}\text{O}$  of for *P. auritum* ( $p < 0.001$ ), no clear effect was found for *C. fairchildiana*. The disagreement of  $\delta^2\text{H}$ -values was increasing with drought for both species ( $p < 0.001$ ).

Moving averages over 2–5 days of  $\delta_{\text{T}}$ -values (Supporting Information: Figure S4) suggest that using an average of several days will account for possible effects of drought and related nonsteady-state effects of transpiration. In addition, flux-weighted daily means of  $\delta_{\text{T}}$ -values consider the mass flux of transpiration and observed diurnal pattern of  $\delta_{\text{T}}$ -values (Figure 3). Using a moving average (here 3 days) of daily flux-weighted  $\delta_{\text{T}}$ -values yielded high-temporal resolution  $\delta_{\text{X}}$ -values that fit well to the isotopic range of soil water across all soil depths for  $\delta^{18}\text{O}$ -values (Figure 7). While transpiration-derived predrought values of  $\delta^{18}\text{O}_{\text{X}}$  matched the isotopic signal of rain source water (the only source water of the rainforest), CVE-derived values were markedly higher for both species. In contrast, transpiration-derived  $\delta^2\text{H}_{\text{X}}$ -values of both species were relatively high compared to source water, in particular for *P. auritum* under drought conditions.

## 4 | DISCUSSION

The isotopic composition of xylem water provides valuable information on the water source of plants and is therefore of considerable interest in ecohydrological research. Using flow-through leaf

chambers, we tested whether the isotopic composition of transpiration may deliver a good proxy for xylem water under varying environmental conditions. In-situ transpiration measurements enabled us to trace dynamics in plant water uptake and use of two tropical plant species, *P. auritum* and *C. fairchildiana*, during increasing drought and subsequent rewetting. As a consequence of drought stress, both species reduced their transpiration rates but differed considerably in their response in  $\delta_{\text{T}}$ -values. While  $\delta_{\text{T}}$ -values of shallow-rooted *P. auritum* increased with increasing drought,  $\delta_{\text{T}}$ -values of deep-rooted *C. fairchildiana* remained relatively stable, suggesting different water sources for *P. auritum* and *C. fairchildiana*. For  $\delta^{18}\text{O}$ , transpiration-derived xylem water values of both species were in the range of the rainforest's water source values, also under drought conditions (Figure 7a). For  $\delta^2\text{H}$ , transpiration-derived xylem water values of both species were relatively high compared to source water. Transpiration-derived values were significantly different from CVE-derived values. While CVE-derived values for  $\delta^{18}\text{O}_{\text{X}}$  were mostly higher, values of  $\delta^2\text{H}_{\text{X}}$  were mostly lower than transpiration-derived values.

### 4.1 | Impact of drought and rewetting on $\delta_{\text{T}}$ and $\delta_{\text{CVE}}$

Experimental drought caused a strong decline in SWC and an increase in VPD in the model tropical rainforest (Figure 1), triggering a pronounced response in  $T$  and  $g_s$  for both species (Figure 2).

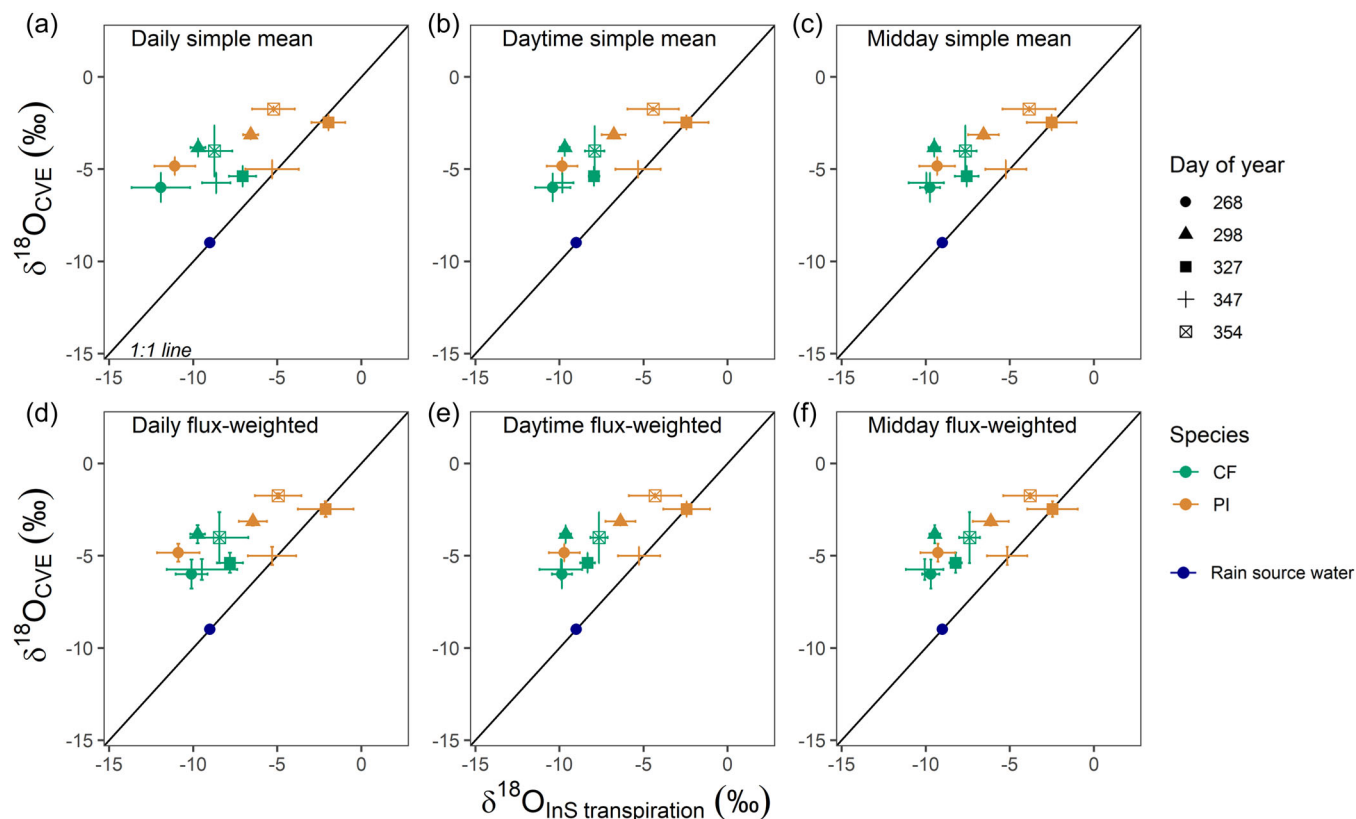


**FIGURE 5** Comparison of the oxygen isotopic composition of xylem water ( $\delta^{18}\text{O}$ , ‰<sub>VSMOW</sub>) derived from in-situ transpiration (InS transpiration) and cryogenic vacuum extraction (CVE).  $\delta^{18}\text{O}_{\text{InS}}$  was calculated based on six approaches: (a) daily simple mean, (b) daytime simple mean, (c) midday simple mean, (d) daily flux-weighted mean, (e) daytime flux-weighted mean and (f) midday flux-weighted mean. Blue dot:  $\delta^{18}\text{O}$  of rain source water. Black line: 1:1 line. Day of year (shape): Time point of destructive sampling. Mean  $\pm$  SE. CF (green), *Clitoria fairchildiana*; PI (brown), *Piper auritum*, VSMOW, Vienna Standard Mean Ocean Water. [Color figure can be viewed at [wileyonlinelibrary.com](https://onlinelibrary.wiley.com/doi/10.1111/pce.14475)]

Dynamics in  $\delta_T$ -values are strongly driven by changes in VPD and closely linked to  $g_s$  (Dubbert et al., 2014a; Lai et al., 2006; Simonin et al., 2013; Wang et al., 2012). We observed strong diurnal variations in  $\delta_T$ -values under well-watered conditions, closely linked to variations in  $g_s$ . The diurnal amplitude decreased with decreasing  $g_s$  in response to soil water deficit and increased again with increasing  $g_s$  after the onset of rain (Figure 3). With the increasing drought,  $\delta_S$ -,  $\delta_T$ - and  $\delta_{\text{CVE}}$ -values steadily increased and then decreased again with the onset of rain (Figures 1 and 3). For *P. auritum*, both  $\delta_T$ - and  $\delta_{\text{CVE}}$ -values (Figures 3 and 4) were generally higher than for *C. fairchildiana*. Evaporative enrichment can occur along the stem (Martín-Gómez et al., 2017; Vega-Grau et al., 2021), affecting in particular less suberized plant species such as *P. auritum*. Higher values of *P. auritum* for  $\delta_T$ - and  $\delta_{\text{CVE}}$ -values can also indicate plant water uptake from more shallow soil layers. The long-term enrichment of  $\delta_T$ - and  $\delta_{\text{CVE}}$ -values observed for *P. auritum* (Figures 2 and 4) with ongoing drought was likely related to the uptake of shallow soil water, subject to evaporative enrichment due to drought (Figure 1c,d).  $\delta_T$ - and  $\delta_{\text{CVE}}$ -values of deeper rooted *C. fairchildiana* increased only slightly during drought and its access to deep water from the bottom soil layers was confirmed when the  $^2\text{H}_2\text{O}$ -pulse led to a strong increase in  $\delta^2\text{H}_T$ - as well as  $\delta^2\text{H}_{\text{CVE}}$ -values.  $\delta^2\text{H}_T$ -values of

*C. fairchildiana* were increasing rapidly  $\sim 2$  days after the  $^2\text{H}_2\text{O}$ -pulse ( $+20.7\text{‰}$  per day, Figure 2d).  $\delta^2\text{H}_T$ -values of *P. auritum* also increased, but the response occurred  $\sim 10$  days after the pulse and was less pronounced ( $+5.1\text{‰}$  per day).  $\delta_T$ -values can be used as a good indicator for water uptake depths and dynamics, particularly when applying water pulses clearly distinguishable in their isotopic composition from the natural source water. Adding an artificial water label strongly increased the variability in  $\delta^2\text{H}_T$ - and  $\delta^2\text{H}_{\text{CVE}}$ -values by amplifying natural variation, which has also been observed in other labelling studies (e.g., Kübert et al., 2020).

## 4.2 | Deriving $\delta_X$ from $\delta_T$ and comparison to CVE and source water

We derived proxies for  $\delta_X$  from  $\delta_T$ -values based on two different approaches, a simple mean and a flux-weighted mean approach, and applied them to different measurement time periods: the daily, daytime and midday period. Comparing transpiration- with CVE-derived values, all approaches delivered a relatively good agreement of  $\delta^{18}\text{O}_X$ -values for *P. auritum* (Figure 5). Midday- and daytime-based values may have fit to CVE-derived values better (mean difference:

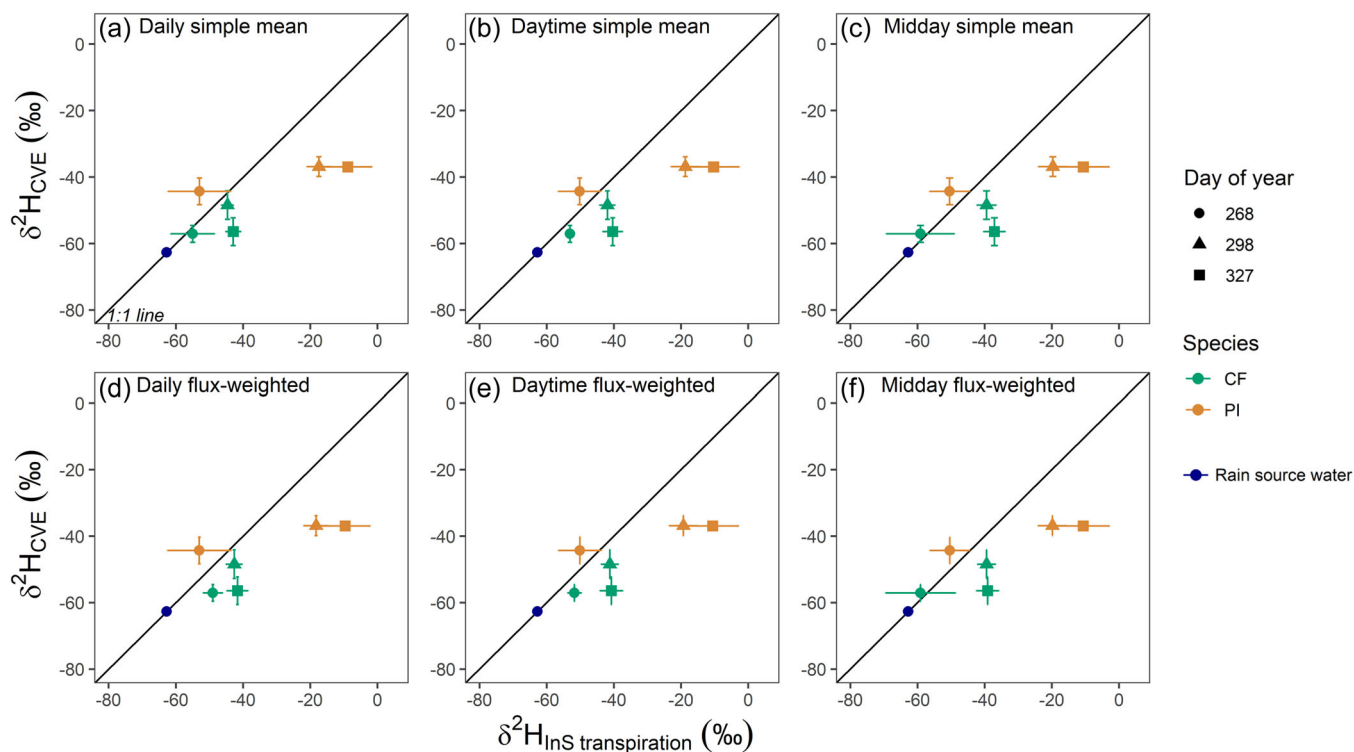


**FIGURE 6** Comparison of the hydrogen isotopic composition of xylem water ( $\delta^2\text{H}$ , ‰<sub>VSMOW</sub>) derived from in-situ transpiration (InS transpiration) and cryogenic vacuum extraction (CVE).  $\delta^2\text{H}_{\text{InS}}$  was calculated based on six approaches: (a) daily simple mean, (b) daytime simple mean, (c) midday simple mean, (d) daily flux-weighted mean, (e) daytime flux-weighted mean and (f) midday flux-weighted mean. Blue dot:  $\delta^2\text{H}$  of rain source water. Black line: 1:1 line. Day of year (shape): Time point of destructive sampling. Mean  $\pm$  SE.  $\delta^2\text{H}$  data from before  $^2\text{H}_2\text{O}$ -pulse, for all data see Supporting Information: Figure S3. CF (green), *Clitoria fairchildiana*; PI (brown), *Piper auritum*; VSMOW, Vienna Standard Mean Ocean Water. [Color figure can be viewed at [wileyonlinelibrary.com](https://onlinelibrary.wiley.com/doi/10.1111/pce.14475)]

**TABLE 1** Differences ( $\Delta$ ) between xylem water isotopic composition derived from CVE and in-situ transpiration

Species	Approach	Time period	Before $^2\text{H}_2\text{O}$ -pulse				All data	
			$\Delta\delta^{18}\text{O}$		$\Delta\delta^2\text{H}$		$\Delta\delta^2\text{H}$	
			Mean	Range	Mean	Range	Mean	Range
CF	Flux-weighted	Daily	4.1	2.4 to 5.9	9.6	-14.8 to -5.9	92.4	-14.8 to 411.6
CF	Flux-weighted	Daytime	4.1	2.9 to 5.8	9.5	-15.8 to -5.4	90.5	-15.8 to 412.5
CF	Flux-weighted	Midday	4.0	2.8 to 5.6	9.5	-17.4 to 1.9	91.4	-17.4 to 417.0
CF	Simple mean	Daily	4.2	1.7 to 5.9	<b>6.5</b>	-13.6 to -2.1	89.2	-13.6 to 409.9
CF	Simple mean	Daytime	4.1	2.5 to 5.8	8.9	-16.1 to -4.1	89.6	-16.1 to 411.4
CF	Simple mean	Midday	<b>3.9</b>	2.2 to 5.7	10.1	-19.4 to 2.0	91.8	-19.4 to 416.8
PI	Flux-weighted	Daily	2.6	-0.4 to 6.0	18.2	-27.4 to 8.6	29.6	-27.4 to 60.7
PI	Flux-weighted	Daytime	2.2	0.0 to 4.9	16.6	-26.4 to 5.8	28.7	-26.4 to 61.0
PI	Flux-weighted	Midday	<b>1.9</b>	0.0 to 4.4	<b>16.5</b>	-26.4 to 6.0	28.4	-26.4 to 61.6
PI	Simple mean	Daily	2.8	-0.5 to 6.2	18.8	-28.2 to 8.6	29.6	-28.2 to 60.1
PI	Simple mean	Daytime	2.3	0.0 to 5.0	16.9	-26.7 to 5.8	28.8	-26.7 to 60.7
PI	Simple mean	Midday	2.0	0.0 to 4.5	16.6	-26.4 to 6.1	28.4	-26.4 to 61.5

Note: This table shows per species, transpiration approach and time period. Data for  $\delta^2\text{H}$  are presented as values before  $^2\text{H}_2\text{O}$ -pulse and all data. Mean of absolute differences and range of differences (including sign). The lowest mean values of  $\Delta\delta^{18}\text{O}$  and  $\Delta\delta^2\text{H}$  (before pulse) per species are given in bold. Abbreviations: CF, *Clitoria fairchildiana*; CVE, cryogenic vacuum extraction; PI, *Piper auritum*.

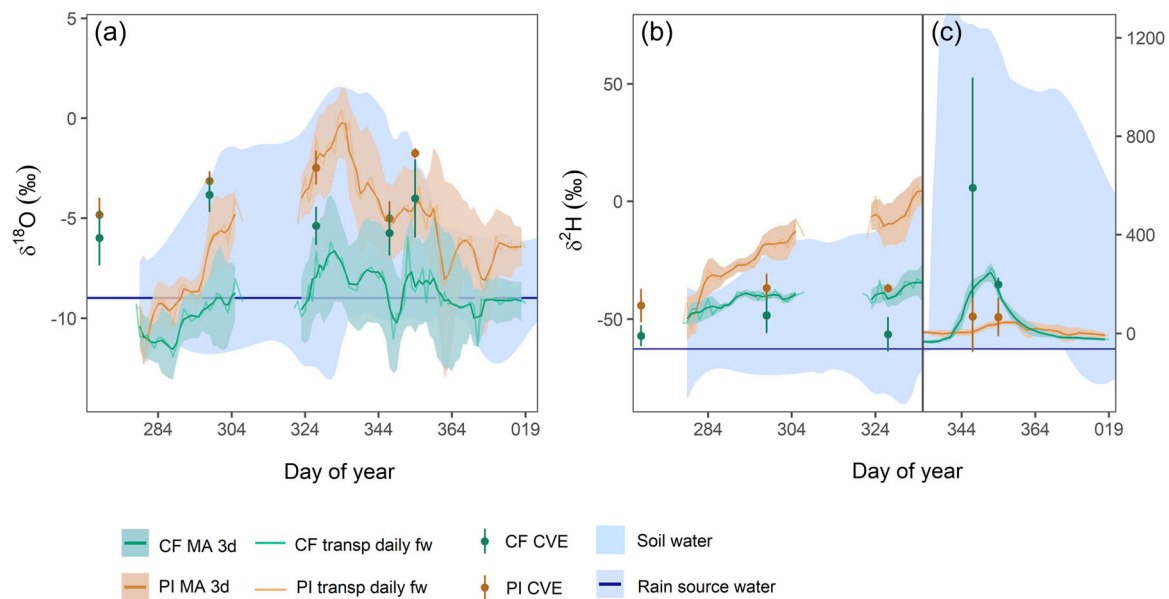


**FIGURE 7** Isotopic composition of xylem water derived from in-situ transpiration (daily flux-weighted [fw] mean and 3-day moving averages [MA 3d]  $\pm$  SD of fw daily mean, lines), and cryogenic vacuum extraction (CVE, dots), for *Clitoria fairchildiana* (CF, green) and *Piper auritum* (PI, brown) (mean  $\pm$  SD). Isotopic composition of soil water (blue shading, based on min/max range of  $\delta_s$ -values) and the rain source water (dark blue line, mean  $\pm$  SE). (a) Oxygen isotopic composition ( $\delta^{18}\text{O}$ , ‰<sub>VSMOW</sub>) and hydrogen isotopic composition ( $\delta^2\text{H}$ , ‰<sub>VSMOW</sub>) before  $^2\text{H}_2\text{O}$ -pulse (b) and after (c). Note the different scales for (b) and (c). VSMOW, Vienna Standard Mean Ocean Water.

1.9‰ vs. 2.2‰; Table 1) since branch sampling took place during midday. The isotopic composition of branch xylem water may also underly strong diurnal variation (De Deurwaerder et al., 2020; Magh et al., 2020; Zhao et al., 2016).

For *C. fairchildiana*, the differences between CVE and transpiration method were larger (3.9‰–4.2‰; Table 1), which could be attributed to the sampling of different branches at each time point, the widespread spatial distribution of measured individuals within the model rainforest, and their large variation in height. In case of *P. auritum*, all leaves were sampled at a height of 3–4 m, and three out of four individual plants were located in the same area ( $\sim 4\text{ m}^2$ ). *C. fairchildiana* also exhibited lower  $g_s$ -values in the initial drought phase than *P. auritum*, which might indicate increasing stomatal closure in response to drought stress leading to nonsteady-state transpiration. However, isotopic nonsteady-state effects on  $\delta_T$ -values need to be eventually compensated, that is, high  $\delta_T$ -values are inevitably followed by low values, and vice versa (Figure 3). Highly enriched or depleted values can only occur over short time-scales, that is, hours or, in extreme cases, days (Dubbert et al., 2014a). Therefore, when averaging measurements over longer time periods (here 3 days), isotopic nonsteady-state effects are likely to even out.

Generally, transpiration-derived  $\delta^{18}\text{O}_X$ -values resembled rain and soil water of the rainforest better than CVE-derived values (Figure 7a). The markedly higher  $\delta^{18}\text{O}$ -values of CVE in comparison to rain source water during predrought conditions when the isotopic effect of soil evaporation was minor are noteworthy.

$\delta^2\text{H}_X$ -values from CVE were mostly depleted in  $^2\text{H}$  compared to transpiration-derived  $\delta^2\text{H}_X$ -values, in particular during drought (for all

approaches; Figure 6), as reported in numerous studies and discussed recently in detail (see Allen & Kirchner, 2021; Barbata et al., 2022; Chen et al., 2020). Chen et al. (2020) showed strong depleting isotopic effects of CVE on  $\delta^2\text{H}$  of up to  $-11\text{‰}$ , possibly due to an exchange between organically (e.g., cellulose) and water molecule-bound Barbata et al. (2022) found even an offset of  $-16\text{‰}$  and explained this by isotopic heterogeneity in bulk stem water. They observed that nonconductive xylem tissue was depleted in  $^2\text{H}$  by on average  $-24\text{‰}$  relative to sap water, that is, CVE of xylem samples may include depleted xylem water that does not contribute to sap flow and thus transpiration, causing a depleted xylem water signal relative to sap and source water. In our study, differences between CVE- and transpiration-derived values increased with drought and were more pronounced for the nonwoody-species *P. auritum*, with a deviation of up to  $-34\text{‰}$  (Figure 6). CVE-derived  $\delta^2\text{H}_X$ -values were within the range of soil water. Transpiration-derived  $\delta^2\text{H}_X$ -values, on the other hand, were relatively high in comparison to rain source water and exceeded soil water values for *P. auritum* during drought (Figures 6 and 7b,c).

Observed differences between transpiration- and CVE-derived values could be also attributed to fractionation effects during transport or redistribution within the plant (Vega-Grau et al., 2021; Zhao et al., 2016). This is particularly relevant for nonwoody, that is, less suberized, species but would affect  $\delta^{18}\text{O}_X$ -values as well. Here, transpiration-derived  $\delta^{18}\text{O}_X$ -values were lower and  $\delta^2\text{H}_X$ -values higher than CVE-derived results. Fractionation effects can also occur during plant water uptake (Poca et al., 2019) but affect xylem water and transpired water isotopes equally. Moreover, the observed offset



in  $\delta^2\text{H}$  could be species-specific and/or depend on the laboratory's extraction procedures (Allen & Kirchner, 2021; Barbeta et al., 2022; Chen et al., 2020). Indeed, we found a better match for *C. fairchildiana* than for *P. auritum* (Table 1 and Figure 6), suggesting a species-specific influence.

The observed isotopic effects of CVE on  $\delta^2\text{H}$ -values are of particular importance for natural abundance isotope studies. By applying water of 'artificial' isotopic composition and hence increasing isotopic differences between different water sources, these effects are minor when studying, for instance, plant water uptake depths.  $\delta^{18}\text{O}$ -values, on the other hand, seem less affected by CVE (Allen & Kirchner, 2021; Chen et al., 2020) and showed a relatively good agreement of in-situ transpiration and CVE-derived data for *P. auritum* (Figure 5).

Transpiration-derived  $\delta^{18}\text{O}_\text{x}$ -values matched rain and soil water better than CVE-derived values (Figure 7a). Our results, therefore, suggest that transpiration-derived xylem water isotope values may provide a more robust proxy for  $\delta^{18}\text{O}_\text{x}$ -values, due to its better time resolution, increasing sampling frequency and thus data availability, and by avoiding potential methodological constraints regarding CVE. However, it must be noted that in-situ isotopic measurements of transpired water are also error-prone. Possible fractionation effects could occur directly after enclosing the leaves in the chambers or whenever water condenses in the tubing.

An important advantage of using the in-situ transpiration method is that we could derive one value of xylem water isotopic composition every day from each plant individual, spanning a time frame of more than 60 days. To reach the same temporal resolution with the destructive approach, we would have needed to collect plant samples on 60 days multiplied by 4 individuals for each species, that is, in total 480 samples resulting in cost- and labour-intensive work in the laboratory (Kübert et al., 2020) and entailing a massive impact on the rainforest's biomass. Moreover, in case of the herbaceous species *P. auritum*, this quantity of destructive samples would be impossible as it is a relatively small plant compared to *C. fairchildiana* and with only a few broad leaves per stalk. A daily temporal resolution though is, for instance, needed to resolve the response patterns of plant water uptake and use to forthcoming rain events.

Generally, the flux-weighted mean approach provided the best proxy for  $\delta^{18}\text{O}_\text{x}$ -values and differences between daily, daytime and midday time periods were small, likely because the flux-weighted mean approach accounted for the mass flux of transpiration that is usually higher during midday than at other times of the day. Our results imply that the role of nonsteady-state transpiration for  $\delta_\text{T}$ -values is minor when considering the time with the highest transpiration rates and that  $\delta^{18}\text{O}_\text{T}$  can serve as proxy for  $\delta^{18}\text{O}_\text{x}$ -values for times of high transpiration and vice versa. Therefore, monitoring midday values could be sufficient to account for possible nonsteady state transpiration effects as long as the time with the highest transpiration rates is included, as also found in other studies (Lee et al., 2007; Welp et al., 2008).

For  $\delta^2\text{H}$ -values, none of the approaches delivered a good agreement with CVE-derived values. The weaker agreement of

transpiration- and CVE-derived xylem water values for  $\delta^2\text{H}$  may be attributed to CVE effects. Though,  $\delta^2\text{H}$ -values of transpiration were relatively high in comparison to rain and soil water, in particular during plant drought stress. More research is needed to understand  $\delta^2\text{H}$ -dynamics in transpiration and associated with CVE, observed here and in numerous other studies (e.g., Allen & Kirchner, 2021; Chen et al., 2020; Li et al., 2021; Orlowski et al., 2016, 2018).

To derive a more robust proxy of the xylem water isotopic composition under natural abundance conditions, we suggest using a moving average of at least 3 days to account for possible isotopic nonsteady-state effects of  $\delta_\text{T}$ -values and recommend applying the flux-weighted mean approach, since it considers both mass and isotopic changes of the transpired water and delivered the best fit with CVE-derived  $\delta^{18}\text{O}$ -values. Short-term or snapshot measurements are more likely influenced by isotopic nonsteady-state transpiration than longer-term measurements. Since isotopic nonsteady-state effects on  $\delta_\text{T}$ -values need to be eventually compensated (Dubbart et al., 2014a), averaging measurements over longer time periods will average out isotopic nonsteady-state effects.

### 4.3 | Impact of drought and rewetting on the relationship of $\delta_\text{T}$ and $\delta_\text{CVE}$

With ongoing drought, the impact of a nonsteady state on the isotopic composition of transpiration can increase (Dubbart et al., 2014a), and therefore the observed offset between CVE- and transpiration-derived values for the xylem water isotopic composition may be larger. By comparing 3-day averages of  $\delta_\text{T}$ -values, we accounted for possible nonsteady-state effects. We found that with ongoing drought, the diurnal amplitude of  $\delta_\text{T}$ -values decreased with decreasing diurnal amplitude of  $T$  and  $g_s$ . Drought did not worsen the agreement of both methods for  $\delta^{18}\text{O}$ -values. However, the agreement of both methods significantly declined with drought for  $\delta^2\text{H}$ -values ( $p < 0.001$ ). A good match of  $\delta^2\text{H}$ -values was found under predrought conditions and the agreement of CVE- and transpiration-derived values decreased with increasing drought. On the other hand, also CVE results might be affected by drought stress. CVE-depleting isotopic effects due to  $^2\text{H}$  exchange can be expressed strongly under lower stem water contents than under well-water conditions (Chen et al., 2020). Nevertheless, transpiration-derived  $\delta^2\text{H}_\text{x}$ -values of both species were relatively high during drought in comparison to soil water, especially for *P. auritum*, indicating significant isotopic effects of drought (stress) on  $\delta^2\text{H}$ -values of transpiration. Though the  $\delta^2\text{H}$ -dynamics also reflected the observed isotopic enrichment of transpiration for both species during drought as observed for  $\delta^{18}\text{O}_\text{x}$ -values (Figure 7).

Under drought stress, plants might mobilize plant water pools, such as stem water storage or less mobile leaf water pools, to sustain transpiration (Epila et al., 2017). Consequently, transpiration may be fed by water uptaken and stored at previous time periods that differed in their isotopic composition from more recent plant water uptake and xylem water (Barbeta et al., 2019; Simonin et al., 2013).

This, however, would affect both isotopes, and the increasing disagreement between the two methods with drought was only observed for  $\delta^2\text{H}$ -values. Moreover, due to the design of the model rainforest, the isotopic composition of irrigation and thus those of the plant source water varied only slightly over time. Therefore, observed differences between CVE- and transpiration-derived xylem water results for  $\delta^2\text{H}$  are unlikely attributed to actual differences between transpiration and xylem water. A small offset can also arise from the delay of water transport from the xylem water to the site of transpiration. Xylem samples for CVE were collected from branches at a similar height as the leaf chambers. The distance from branch xylem water to the site of transpiration was relatively small (approx. 10–50 cm, dependent on the distance of leaves to sampled branches) and therefore the related temporal delay likely short (<1 day). A possible delay was also accounted for by comparing an average of transpiration-derived values over several days after the destructive sampling.

Generally, transpiration (its flux and isotopic composition) may vary among leaves within a plant individual, closely linked to a strong spatial as well as temporal variation of xylem water (both flux and isotopic composition) in the stem and branches (Barbeta et al., 2020; De Deurwaerder et al., 2020; Lehnebach et al., 2018; Zhao et al., 2016). By always measuring the same leaf, this natural heterogeneity can be reduced. This facilitates a better observation of underlying mechanisms and drivers, that is, we can distinguish natural isotopic variation among leaves from actual isotopic changes due to, for instance, different plant water uptake depths or the use of different water pools within the plant. In addition, as  $\delta_{\text{T}}$ -values may be influenced by other plant water pools than  $\delta_{\text{X}}$ -values (Aasamaa et al., 2005; Barbour et al., 2021; Steudle et al., 1993; Zwieniecki et al., 2007), combining in-situ high temporal resolution isotopic measurements of both  $\delta_{\text{X}}$ - and  $\delta_{\text{T}}$ -values may enable interesting studies of plant water storages and within-plant (re)distribution of water sources and pools. Moreover, measuring  $\delta_{\text{T}}$ -values directly avoids assumptions and indirect estimates via xylem or leaf water, as often done when, for instance, partitioning ET using water stable isotopes (e.g., Adkison et al., 2020; Kübert et al., 2019).

#### 4.4 | Implications for application

The in-situ transpiration method requires a more complex on-site infrastructure compared to destructive sampling and is limited in its coverage of spatial extent. Yet, the initial investments of time and expertise for the setup of the in-situ method will yield real-time and high temporal resolution measurements and lower operating costs, in particular, if the measurements are automated (Kübert et al., 2020). It is also important to mention that overheating of chambers needs to be avoided (e.g., through ventilation and temperature control) and that instead of self-built chambers, leaf cuvettes from commercial gas exchange systems could be used to determine  $\delta_{\text{T}}$ -values (see, e.g., Dubbert et al., 2017). Moreover, combining in-situ transpiration measurements with destructive xylem sampling for isotopic analysis,

taking place for instance at the beginning and/or at the end of an experiment, may allow both temporal dynamics and spatial heterogeneity of plant and ecosystem responses to be determined.

In addition, more and more ecohydrological studies now apply in-situ methods to derive soil water isotopic composition, based on soil water vapour measurements (e.g., Kühnhammer et al., 2020, 2022; Oerter & Bowen, 2019; Seeger & Weiler, 2021). Using the same water isotope analyser or similar type for measurements of soil and transpired water vapour can minimize instrument- and calibration-related isotopic discrepancies. Applying the in-situ transpiration method may therefore be methodologically more stringent than CVE when comparing derived soil and plant water isotope data.

The most important advantage of in-situ transpiration measurements, however, is that this method can be used for any vegetation type or growth form, nonwoody and woody plants, whose leaves or leaf-like structures can be enclosed and separated from soils. Whereas much research and effort has been placed on the improvements of in-situ isotope methods for tree species and forest ecosystems to determine water sources of trees, only few studies have dealt with the water use and uptake of herbaceous species and grassland ecosystems using in-situ isotope methods (e.g., Kübert et al., 2019; Kühnhammer et al., 2020). Due to their nonwoody structure, methods, such as the xylem equilibration method within stems (Marshall et al., 2020; Volkmann et al., 2016), cannot be applied to nonwoody plants and xylem water can only be accessed destructively with a large impact on small plants. A large part of the Earth's terrestrial (agro)ecosystems are solely composed or dominated by nonwoody species (Buchhorn et al., 2020), and they can also contribute significantly to ecosystem water fluxes in forested areas, for example, as observed in savanna-type ecosystems (Dubbert et al., 2014b). Using in-situ transpiration measurements for isotope approaches are therefore an ideal tool to study the role and functioning of nonwoody species in ecosystem water cycling, a crucial and large knowledge gap that urgently needs to be filled.

## 5 | CONCLUSION

Here, we tested the suitability of gas exchange chamber measurements to derive the xylem water isotopic composition at a high temporal resolution, using a nondestructive method that is not limited to woody species. We found that  $\delta_{\text{T}}$ -values are a clear indicator for  $\delta_{\text{X}}$ -dynamics, even under drought conditions. We were able to retrieve data at a high temporal resolution for both  $\delta_{\text{T}}$ - and  $\delta_{\text{X}}$ -values over long time periods for a tree and an herbaceous species, which would have been infeasible by traditional destructive approaches. While transpiration-derived  $\delta^{18}\text{O}_{\text{X}}$ -values matched those of source water,  $\delta^2\text{H}_{\text{X}}$ -values were in comparison relatively high. CVE-derived values for  $\delta^{18}\text{O}_{\text{X}}$  were mostly higher, values of  $\delta^2\text{H}_{\text{X}}$  were mostly lower than transpiration-derived values. Our results, therefore, suggest caution when using CVE-derived xylem water values as an isotopic proxy for transpiration. More research is

needed to understand the underlying  $\delta^2\text{H}$ -dynamics of transpired and xylem water.

In-situ transpiration isotopic measurements are a valuable method to directly derive  $\delta_T$ -values for isotope-based ET partitioning. The additional information on leaf gas exchange is a big advantage of direct measurements of transpiration. Plant responses in gas exchange and  $\delta_T$ -values can be observed in-situ, resolve high-resolution temporal dynamics and indicate plant water stress. Our method is applicable to a wide range of woody and nonwoody plant species and growth forms and opens up new opportunities to study plant water uptake in particular in combination with artificially enriched or depleted isotope tracers.

## ACKNOWLEDGEMENTS

We thank all members of the B2WALD team for their valuable support (please see [https://arizona.figshare.com/articles/dataset/B2WALD\\_Campaign\\_Team\\_and\\_Contributions/14632662/2](https://arizona.figshare.com/articles/dataset/B2WALD_Campaign_Team_and_Contributions/14632662/2)) and special thanks to Jason Deleeuw, Sydney Kerman, Erik Daber and Johannes Ingrisich for support and advice. We also thank two anonymous reviewers for their feedback on this work to improve this manuscript. This work was supported by the European Research Council (ERC consolidator grant #647008 (VOCO<sub>2</sub>) to C. W.), the Phileology Foundation to Biosphere 2 to L. K. M. and the German Research Foundation (DFG grant #DU1688/1-1 to M. D.). Open Access funding enabled and organized by Projekt DEAL.

## CONFLICT OF INTEREST

The authors declare no conflict of interest.

## DATA AVAILABILITY STATEMENT

All data used in this manuscript are publicly available at <https://doi.org/10.6094/UNIFR/230715>.

## ORCID

Angelika Kübert  <http://orcid.org/0000-0003-3985-9261>

Christiane Werner  <http://orcid.org/0000-0002-7676-9057>

## REFERENCES

- Aasamaa, K., Niinemets, Ü. & Söber, A. (2005) Leaf hydraulic conductance in relation to anatomical and functional traits during *Populus tremula* leaf ontogeny. *Tree Physiology*, 25, 1409–1418. Available from: <https://doi.org/10.1093/treephys/25.11.1409>
- Adkison, C., Cooper-Norris, C., Patankar, R. & Moore, G.W. (2020) Using high-frequency water vapor isotopic measurements as a novel method to partition daily evapotranspiration in an oak woodland. *Water*, 12, 2967. Available from: <https://doi.org/10.3390/w12112967>
- Allen, S.T. & Kirchner, J.W. (2021) Potential effects of cryogenic extraction biases on inferences drawn from xylem water deuterium isotope ratios: case studies using stable isotopes to infer plant water sources. *Hydrology and Earth System Sciences Discussions*, 1–15. Available from: <https://doi.org/10.5194/hess-2020-683>
- Barbeta, A., Burlett, R., Martín-Gómez, P., Fréjaville, B., Devert, N., Wingate, L. et al. (2022) Evidence for distinct isotopic compositions of sap and tissue water in tree stems: consequences for plant water source identification. *New Phytologist*, 233, 1121–1132. Available from: <https://doi.org/10.1111/nph.17857>
- Barbeta, A., Gimeno, T.E., Clavé, L., Fréjaville, B., Jones, S.P., Delvigne, C. et al. (2020) An explanation for the isotopic offset between soil and stem water in a temperate tree species. *New Phytologist*, 227, 16564. Available from: <https://doi.org/10.1111/nph.16564>
- Barbeta, A., Jones, S.P., Clavé, L., Wingate, L., Gimeno, T.E., Fréjaville, B. et al. (2019) Unexplained hydrogen isotope offsets complicate the identification and quantification of tree water sources in a riparian forest. *Hydrology and Earth System Sciences*, 23, 2129–2146. Available from: <https://doi.org/10.5194/hess-23-2129-2019>
- Barbour, M.M., Loucos, K.E., Lockhart, E.L., Shrestha, A., McCallum, D., Simonin, K.A. et al. (2021) Can hydraulic design explain patterns of leaf water isotopic enrichment in C3 plants? *Plant, Cell & Environment*, 44, 432–444. Available from: <https://doi.org/10.1111/pce.13943>
- Bates, D., Mächler, M., Bolker, B. & Walker, S. (2015) Fitting linear mixed-effects models using lme4. *Journal of Statistical Software*, 67, 1–48. Available from: <https://doi.org/10.18637/jss.v067.i01>
- Benettin, P., Nehemy, M.F., Cernusak, L.A., Kahmen, A. & McDonnell, J.J. (2021) On the use of leaf water to determine plant water source: a proof of concept. *Hydrological Processes*, 35, e14073. Available from: <https://doi.org/10.1002/hyp.14073>
- Brunel, J.P., Walker, G.R., Dighton, J.C. & Monteny, B. (1997) Use of stable isotopes of water to determine the origin of water used by the vegetation and to partition evapotranspiration. A case study from HAPEX-Sahel. *Journal of Hydrology*, 188–189, 466–481. Available from: [https://doi.org/10.1016/S0022-1694\(96\)03188-5](https://doi.org/10.1016/S0022-1694(96)03188-5)
- Buchhorn, M., Smets, B., Bertels, L., Lesiv, M., Tsendbazar, N.-E. & Masiliunas, D. et al. (2020) *Copernicus global land service: land cover 100 m: collection 3: epoch 2019: globe (version V3.0.1)* [Data set]. Zenodo. Available from: <https://doi.org/10.5281/zenodo.3939050>
- von Caemmerer, S. & Farquhar, G.D. (1981) Some relationships between the biochemistry of photosynthesis and the gas exchange of leaves. *Planta*, 153, 376–387. Available from: <https://doi.org/10.1007/BF00384257>
- Chakraborty, S., Belek, A.R., Datye, A. & Sinha, N. (2018) Isotopic study of intraseasonal variations of plant transpiration: an alternative means to characterise the dry phases of monsoon. *Scientific Reports*, 8, 8647. Available from: <https://doi.org/10.1038/s41598-018-26965-6>
- Chen, Y., Helliher, B.R., Tang, X., Li, F., Zhou, Y. & Song, X. (2020) Stem water cryogenic extraction biases estimation in deuterium isotope composition of plant source water. *Proceedings of the National Academy of Sciences*, 117, 33345–33350. <https://doi.org/10.1073/pnas.2014422117>
- De Duerwaerde, H.P.T., Visser, M.D., Detto, M., Boeckx, P., Meunier, F., Kuehnhammer, K. et al. (2020) Causes and consequences of pronounced variation in the isotope composition of plant xylem water. *Biogeosciences*, 17, 4853–4870. Available from: <https://doi.org/10.5194/bg-17-4853-2020>
- Dongmann, G., Nürnberg, H.W., Förstel, H. & Wägenar, K. (1974) On the enrichment of H<sub>2</sub>18O in the leaves of transpiring plants. *Radiation and Environmental Biophysics*, 11, 41–52. Available from: <https://doi.org/10.1007/BF01323099>
- Dubbert, M., Cuntz, M., Piayda, A., Maguás, C. & Werner, C. (2013) Partitioning evapotranspiration—testing the Craig and Gordon model with field measurements of oxygen isotope ratios of evaporative fluxes. *Journal of Hydrology*, 496, 142–153. Available from: <https://doi.org/10.1016/j.jhydrol.2013.05.033>
- Dubbert, M., Cuntz, M., Piayda, A. & Werner, C. (2014a) Oxygen isotope signatures of transpired water vapor: the role of isotopic non-steady-state transpiration under natural conditions. *New Phytologist*, 203, 1242–1252. Available from: <https://doi.org/10.1111/nph.12878>

- Dubbert, M., Kübert, A. & Werner, C. (2017) Impact of leaf traits on temporal dynamics of transpired oxygen isotope signatures and its impact on atmospheric vapor. *Frontiers in Plant Science*, 8, 5. Available from: <https://doi.org/10.3389/fpls.2017.00005>
- Dubbert, M., Piayda, A., Cuntz, M., Correia, A.C., Costa e Silva, F. & Pereira, J.S. et al. (2014b) Stable oxygen isotope and flux partitioning demonstrates understory of an oak savanna contributes up to half of ecosystem carbon and water exchange. *Frontiers in Plant Science*, 5, 1–16. Available from: <https://doi.org/10.3389/fpls.2014.00530>
- Dubbert, M. & Werner, C. (2019) Water fluxes mediated by vegetation: emerging isotopic insights at the soil and atmosphere interfaces. *New Phytologist*, 221, 1754–1763. Available from: <https://doi.org/10.1111/nph.15547>
- Ehleringer, J.R. & Dawson, T.E. (1992) Water uptake by plants: perspectives from stable isotope composition. *Plant, Cell & Environment*, 15, 1073–1082. Available from: <https://doi.org/10.1111/j.1365-3040.1992.tb01657.x>
- Ehleringer, J.R. & Osmond, C.B. (1989) Stable isotopes. In: Percy, R.W., Ehleringer, J.R., Mooney, H.A. & Rundel, P.W. (Eds.) *Plant physiological ecology: field methods and instrumentation*. London: Kluwer, pp. 281–300.
- Ehleringer, J.R., Roden, J. & Dawson, T.E. (2000) Assessing ecosystem-level water relations through stable isotope ratio analyses. In: Sala, O.E., Jackson, R.B., Mooney, H.A. & Howarth, R.W. (Eds.) *Methods in Ecosystem Science*. New York, NY: Springer, pp. 181–198. [https://doi.org/10.1007/978-1-4612-1224-9\\_13](https://doi.org/10.1007/978-1-4612-1224-9_13)
- Epila, J., De Baerdemaeker, N., Vergeynst, L.L., Maes, W.H., Beeckman, H. & Steppe, K. (2017) Capacitive water release and internal leaf water relocation delay drought-induced cavitation in African *Maesopsis eminii*. *Tree Physiology*, 37, 481–490. Available from: <https://doi.org/10.1093/treephys/tpw128>
- Fischer, B.M.C., Frentress, J., Manzoni, S., Cousins, S.A.O., Hugelius, G., Greger, M. et al. (2019) Mojito, anyone? An exploration of low-tech plant water extraction methods for isotopic analysis using locally-sourced materials. *Frontiers in Earth Science*, 7, 1–11. Available from: <https://doi.org/10.3389/feart.2019.00150>
- Flanagan, L.B., Comstock, J.P. & Ehleringer, J.R. (1991) Comparison of modeled and observed environmental influences on the stable oxygen and hydrogen isotope composition of leaf water in *Phaseolus vulgaris*. *Plant Physiology*, 96, 588–596. Available from: <https://doi.org/10.1104/pp.96.2.588>
- Förstel, H. (1978) The enrichment of  $^{18}\text{O}$  in leaf water under natural conditions. *Radiation and Environmental Biophysics*, 15, 323–344. Available from: <https://doi.org/10.1007/BF01323459>
- Förstel, H. (1982)  $\delta^{18}\text{O}/^{16}\text{O}$  ratio of water in plants and their environment. In: Schmidt, H.L., Förstel, H. & Heinzinger, K. (Eds.) *Stable isotopes*. Amsterdam: Elsevier, pp. 503–516.
- Gonfiantini, R. (1978) Standards for stable isotope measurements in natural compounds. *Nature*, 271, 534–536.
- Horita, J. & Wesolowski, D.J. (1994) Liquid-vapor fractionation of oxygen and hydrogen isotopes of water from the freezing to the critical temperature. *Geochimica et Cosmochimica Acta*, 58, 3425–3437. Available from: [https://doi.org/10.1016/0016-7037\(94\)90096-5](https://doi.org/10.1016/0016-7037(94)90096-5)
- Kübert, A., Götz, M., Kuester, E., Piayda, A., Werner, C. & Rothfuss, Y. et al. (2019) Nitrogen loading enhances stress impact of drought on a semi-natural temperate grassland. *Frontiers in Plant Science*, 10, 1051. Available from: <https://doi.org/10.3389/fpls.2019.01051>
- Kübert, A., Paulus, S., Dahlmann, A., Werner, C., Rothfuss, Y. & Orłowski, N. et al. (2020) Water stable isotopes in ecohydrological field research: comparison between in situ and destructive monitoring methods to determine soil water isotopic signatures. *Frontiers in Plant Science*, 11, 387. Available from: <https://doi.org/10.3389/fpls.2020.00387>
- Kühnhammer, K., Dahlmann, A., Iraheta, A., Gerchow, M., Birkel, C., Marshall, J.D. et al. (2022) Continuous in situ measurements of water stable isotopes in soils, tree trunk and root xylem: field approval. *Rapid Communications in Mass Spectrometry*, 36, e9232. Available from: <https://doi.org/10.1002/rcm.9232>
- Kühnhammer, K., Kübert, A., Brüggemann, N., Deseano Diaz, P., Dusschoten, D., Javaux, M. et al. (2020) Investigating the root plasticity response of *Centaurea jacea* to soil water availability changes from isotopic analysis. *New Phytologist*, 226, 98–110. Available from: <https://doi.org/10.1111/nph.16352>
- Kulmatiski, A. & Forero, L.E. (2021) Bagging: a cheaper, faster, non-destructive transpiration water sampling method for tracer studies. *Plant and Soil*, 462, 603–611. Available from: <https://doi.org/10.1007/s11104-021-04844-w>
- Kuznetsova, A., Brockhoff, P.B., Christensen, R.H.B. & Jensen, S.P. (2020) *lmerTest: Tests in Linear Mixed Effects Models*.
- Ladd, S.N. & Sachs, J.P. (2015) Influence of salinity on hydrogen isotope fractionation in Rhizophora mangroves from Micronesia. *Geochimica et Cosmochimica Acta*, 168, 206–221. Available from: <https://doi.org/10.1016/j.gca.2015.07.004>
- Lai, C.-T., Ehleringer, J.R., Bond, B.J. & Paw U, K.T. (2006) Contributions of evaporation, isotopic non-steady state transpiration and atmospheric mixing on the  $\delta^{18}\text{O}$  of water vapour in Pacific Northwest coniferous forests. *Plant, Cell and Environment*, 29, 77–94. Available from: <https://doi.org/10.1111/j.1365-3040.2005.01402.x>
- Lee, X., Kim, K. & Smith, R. (2007) Temporal variations of the  $^{18}\text{O}/^{16}\text{O}$  signal of the whole-canopy transpiration in a temperate forest. *Global Biogeochemical Cycles*, 21, 1–12. Available from: <https://doi.org/10.1029/2006GB002871>
- Lehnebach, R., Beyer, R., Letort, V. & Heuret, P. (2018) The pipe model theory half a century on: a review. *Annals of Botany*, 121, 773–795. Available from: <https://doi.org/10.1093/aob/mcx194>
- Li, Y., Ma, Y., Song, X., Wang, L. & Han, D. (2021) A  $\delta^2\text{H}$  offset correction method for quantifying root water uptake of riparian trees. *Journal of Hydrology*, 593, 125811. Available from: <https://doi.org/10.1016/j.jhydrol.2020.125811>
- Magh, R.-K., Eiferle, C., Burzlaff, T., Dannenmann, M., Rennenberg, H. & Dubbert, M. (2020) Competition for water rather than facilitation in mixed beech-fir forests after drying-wetting cycle. *Journal of Hydrology*, 587, 124944. Available from: <https://doi.org/10.1016/j.jhydrol.2020.124944>
- Majoube, M. (1971) Oxygen-18 and deuterium fractionation between water and steam (in French). *Journal of Physical Chemistry and Biological Physico-Chemistry*, 68, 1423–1436.
- Marshall, J.D., Cuntz, M., Beyer, M., Dubbert, M. & Kuehnhammer, K. (2020) Borehole equilibration: testing a new method to monitor the isotopic composition of tree xylem water in situ. *Frontiers in Plant Science*, 11, 358. Available from: <https://doi.org/10.3389/fpls.2020.00358>
- Martín-Gómez, P., Serrano, L. & Ferrio, J.P. (2017) Short-term dynamics of evaporative enrichment of xylem water in woody stems: implications for ecohydrology. *Tree Physiology*, 37, 511–522. Available from: <https://doi.org/10.1093/treephys/tpw115>
- McDonnell, J.J. (2014) The two water worlds hypothesis: ecohydrological separation of water between streams and trees. *WIREs Water*, 1, 323–329. Available from: <https://doi.org/10.1002/wat2.1027>
- Menchaca, L.B., Smith, B.M., Connolly, J., Conrad, M. & Emmett, B. (2007) A method to determine plant water source using transpired water. *Hydrology and Earth System Sciences Discussions*, 4, 863–880. <https://doi.org/10.5194/hessd-4-863-2007>
- Oerter, E.J. & Bowen, G. (2017) In situ monitoring of H and O stable isotopes in soil water reveals ecohydrologic dynamics in managed soil systems. *Ecohydrology*, 10, e1841. Available from: <https://doi.org/10.1002/eco.1841>
- Oerter, E.J. & Bowen, G.J. (2019) Spatio-temporal heterogeneity in soil water stable isotopic composition and its ecohydrologic implications



- in semiarid ecosystems. *Hydrological Processes*, 33, 1724–1738. Available from: <https://doi.org/10.1002/hyp.13434>
- Orlowski, N., Breuer, L., Angeli, N., Boeckx, P., Brumbt, C., Cook, C.S. et al. (2018) Inter-laboratory comparison of cryogenic water extraction systems for stable isotope analysis of soil water. *Hydrology and Earth System Sciences*, 22, 3619–3637. Available from: <https://doi.org/10.5194/hess-22-3619-2018>
- Orlowski, N., Frede, H.-G., Brüggemann, N. & Breuer, L. (2013) Validation and application of a cryogenic vacuum extraction system for soil and plant water extraction for isotope analysis. *Journal of Sensors and Sensor Systems*, 2, 179–193. Available from: <https://doi.org/10.5194/jsss-2-179-2013>
- Orlowski, N., Pratt, D.L. & McDonnell, J.J. (2016) Intercomparison of soil pore water extraction methods for stable isotope analysis. *Hydrological Processes*, 30, 3434–3449. Available from: <https://doi.org/10.1002/hyp.10870>
- Rothfuss, Y. & Javaux, M. (2017) Reviews and syntheses: isotopic approaches to quantify root water uptake: a review and comparison of methods. *Biogeosciences*, 14, 2199–2224. Available from: <https://doi.org/10.5194/bg-14-2199-2017>
- Rothfuss, Y., Vereecken, H. & Brüggemann, N. (2013) Monitoring water stable isotopic composition in soils using gas-permeable tubing and infrared laser absorption spectroscopy: monitoring water stable isotopic composition in soils. *Water Resources Research*, 49, 3747–3755. Available from: <https://doi.org/10.1002/wrcr.20311>
- Schmidt, M., Masey, K., Lett, C., Biron, P., Richard, P., Barriac, T. et al. (2010) Concentration effects on laser-based  $\delta^{18}\text{O}$  and  $\delta^2\text{H}$  measurements and implications for the calibration of vapour measurements with liquid standards. *Rapid Communications in Mass Spectrometry*, 24, 3553–3561. Available from: <https://doi.org/10.1002/rcm.4813>
- Seeger, S. & Weiler, M. (2021) Temporal dynamics of tree xylem water isotopes: in situ monitoring and modeling. *Biogeosciences*, 18, 4603–4627. Available from: <https://doi.org/10.5194/bg-18-4603-2021>
- Simonin, K.A., Roddy, A.B., Link, P., Apodaca, R., Tu, K.P., Hu, J. et al. (2013) Isotopic composition of transpiration and rates of change in leaf water isotopologue storage in response to environmental variables. *Plant, Cell & Environment*, 36, 2190–2206. Available from: <https://doi.org/10.1111/pce.12129>
- Sprenger, M., Leistert, H., Gimbel, K. & Weiler, M. (2016) Illuminating hydrological processes at the soil-vegetation-atmosphere interface with water stable isotopes: review of water soluble isotopes. *Reviews of Geophysics*, 54, 674–704. Available from: <https://doi.org/10.1002/2015RG000515>
- Steudle, E., Murrmann, M. & Peterson, C.A. (1993) Transport of water and solutes across maize roots modified by puncturing the endodermis (further evidence for the composite transport model of the root. *Plant physiology*, 103, 335–349. Available from: <https://doi.org/10.1104/pp.103.2.335>
- Tetens, O. (1930) Über einige meteorologische Begriffe. *Zeitschrift für Geophysik*, 6, 297–309.
- Thorburn, P.J., Walker, G.R. & Brunel, J.-P. (1993) Extraction of water from eucalyptus trees for analysis of deuterium and oxygen-18: laboratory and field techniques. *Plant, Cell & Environment*, 16, 269–277. Available from: <https://doi.org/10.1111/j.1365-3040.1993.tb00869.x>
- Vega-Grau, A.M., McDonnell, J., Schmidt, S., Annandale, M. & Herbohn, J. (2021) Isotopic fractionation from deep roots to tall shoots: a forensic analysis of xylem water isotope composition in mature tropical savanna trees. *Science of the Total Environment*, 795, 148675. Available from: <https://doi.org/10.1016/j.scitotenv.2021.148675>
- Volkman, T.H., Kühnhammer, K., Herbstritt, B., Gessler, A. & Weiler, M. (2016) A method for in situ monitoring of the isotope composition of tree xylem water using laser spectroscopy. *Plant, Cell & Environment*, 39, 2055–2063. Available from: <https://doi.org/10.1111/pce.12725>
- Volkman, T.H.M. & Weiler, M. (2014) Continual in situ monitoring of pore water stable isotopes in the subsurface. *Hydrology and Earth System Sciences*, 18, 1819–1833. Available from: <https://doi.org/10.5194/hess-18-1819-2014>
- Wang, L., Good, S.P., Caylor, K.K. & Cernusak, L.A. (2012) Direct quantification of leaf transpiration isotopic composition. *Agricultural and Forest Meteorology*, 154–155, 127–135. Available from: <https://doi.org/10.1016/j.agrformet.2011.10.018>
- Wang, L., Niu, S., Good, S.P., Soderberg, K., McCabe, M.F., Sherry, R.A. et al. (2013) The effect of warming on grassland evapotranspiration partitioning using laser-based isotope monitoring techniques. *Geochimica et Cosmochimica Acta*, 111, 28–38. Available from: <https://doi.org/10.1016/j.gca.2012.12.047>
- Welp, L.R., Lee, X., Kim, K., Griffis, T.J., Billmark, K.A. & Baker, J.M. (2008) DeltaO of water vapour, evapotranspiration and the sites of leaf water evaporation in a soybean canopy. *Plant, Cell & Environment*, 31, 1214–1228. Available from: <https://doi.org/10.1111/j.1365-3040.2008.01826.x>
- Werner, C., Meredith, L.K., Ladd, S.N., Ingrisch, J., Kübert, A., van Haren, J. et al. (2021) Ecosystem fluxes during drought and recovery in an experimental forest. *Science*, 374, 1514–1518. Available from: <https://doi.org/10.1126/science.abj6789>
- West, A.G., Patrickson, S.J. & Ehleringer, J.R. (2006) Water extraction times for plant and soil materials used in stable isotope analysis. *Rapid Communications in Mass Spectrometry*, 20, 1317–1321. Available from: <https://doi.org/10.1002/rcm.2456>
- Williams, D.G., Cable, W., Hultine, K., Hoedjes, J.C.B., Yepez, E.A., Simonneaux, V. et al. (2004) Evapotranspiration components determined by stable isotope, sap flow and eddy covariance techniques. *Agricultural and Forest Meteorology*, 125, 241–258. Available from: <https://doi.org/10.1016/j.agrformet.2004.04.008>
- Wong, S.C. (1979) Elevated atmospheric partial pressure of CO<sub>2</sub> and plant growth. *Oecologia*, 44, 68–74. Available from: <https://doi.org/10.1007/BF00346400>
- Yepez, E.A., Williams, D.G., Scott, R.L. & Lin, G. (2003) Partitioning overstory and understory evapotranspiration in a semiarid savanna woodland from the isotopic composition of water vapor. *Agricultural and Forest Meteorology*, 119, 53–68. Available from: [https://doi.org/10.1016/S0168-1923\(03\)00116-3](https://doi.org/10.1016/S0168-1923(03)00116-3)
- Zhao, L., Wang, L., Cernusak, L.A., Liu, X., Xiao, H., Zhou, M. et al. (2016) Significant difference in hydrogen isotope composition between xylem and tissue water in *Populus Euphratica*. *Plant, Cell & Environment*, 39, 1848–1857. Available from: <https://doi.org/10.1111/pce.12753>
- Zimmermann, U., Ehalt, D. & Muennich, K.O. (1968) *Soil-water movement and evapotranspiration: changes in the isotopic composition of the wafter*. Vienna: International Atomic Energy Agency, pp. 567–585.
- Zwieniecki, M.A., Brodribb, T.J. & Holbrook, N.M. (2007) Hydraulic design of leaves: insights from rehydration kinetics. *Plant, Cell & Environment*, 30, 910–921. Available from: <https://doi.org/10.1111/j.1365-3040.2007.001681.x>

## SUPPORTING INFORMATION

Additional supporting information can be found online in the Supporting Information section at the end of this article.

**How to cite this article:** Kübert, A., Dubbert, M., Bamberger, I., Kühnhammer, K., Beyer, M. van, Haren, J., et al. (2023) Tracing plant source water dynamics during drought by continuous transpiration measurements: an in-situ stable isotope approach. *Plant, Cell & Environment*, 46, 133–149. <https://doi.org/10.1111/pce.14475>